Electronic Supplementary Material (ESI) for Journal of Materials Chemistry C.

Fluorescent Aryl Naphthalene Dicarboximides with Large Stokes' Shifts and Strong Solvatochromism Controlled by Dynamics and Molecular Geometry

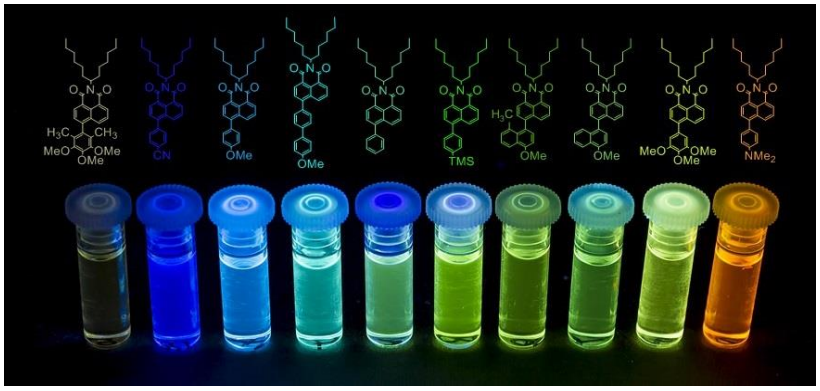

Robert Greiner, Thorben Schlücker[+], Dominik Zgela and Heinz Langhals*

LMU Ludwig-Maximilians-Universität München, Department Chemie

Butenandtstrasse 5-13, Haus F, 81377 München (Germany)

Fax: (+49) 089 2180 77640

e-mail: Langhals@lrz.uni-muenchen.de

Supporting Information

Table of Contents

1. General Information

All reactions were carried out under an argon atmosphere in flame-dried glassware. Syringes which were used to transfer anhydrous solvents or reagents were purged with argon prior to use. Available standard chemicals were applied in synthesis grade without further purification. 1-Butanol, chloroform, hexane and toluene were used in spectrophotometric grade. DMF, tetradecane and 1-undecanol were used in p.a. grade and stored over 3 Å molar sieve. Toluene and THF were continuously refluxed and freshly distilled from sodium benzophenone ketyl under nitrogen and stored over 4 Å molecular sieves. Yields refer to isolated compounds estimated to be > 95 % pure as determined by ^{1}H NMR (25 °C) and capillary GC. Chemical shifts are reported as δ-values in ppm relative to the solvent peak. NMR spectra were recorded in a solution of $CDCl_3$ (residual chloroform: δ = 7.27 ppm for ^{1}H NMR and δ = 77.0 ppm for ^{13}C NMR). Abbreviations for signal coupling are as follows: s, singlet; br s, broad singlet; d, doublet; t, triplet; q, quartet; quin, quintet; sxt, sextet; m, multiplet. Infrared spectra were recorded from 4000-400 cm^{-1} on a Perkin 281 IR spectrometer. Samples were measured neat (ATR, Smiths Detection DuraSample IR II Diamond ATR). The absorption bands were reported in wave numbers (cm^{-1}). Mass Spectra were recorded on Finnigan MAT 95Q or Finnigan MAT 90 instrument for electron impact ionization (EI). High Resolution Mass Spectra (HRMS) were recorded on the same instrument. UV/Vis spectra were obtained with a Varian Cary 5000 spectrometer. Fluorescence spectra were obtained with a Varian Cary Eclipse spectrometer, slit width 2.5 nm. Fluorescence lifetimes τ were obtained with a PicoQuant 300 lifetime spectrometer and a PicoQuant P-C-405 as lightsorce. Column chromatography was performed using SiO_2 (0.040 – 0.063 mm, 230 – 400 mesh ASTM) from Merck if not indicated. All reagents were obtained from commercial sources and used without further purification if not otherwise stated.

2. Preparation of aryl dioxaborolanes

4-(Trimethylsilyl)phenylboronic acid and the pinacol esters of phenylboronic acid, 4-methoxyphenylboronic acid, 4-(*N,N*-dimethylamino)phenylboronic acid and 4-cyanophenylboronic acid have been purchased from commercial sources.

2-(4-Methoxynaphthalen-1-yl)-4,4,5,5-tetramethyl-1,3,2-dioxaborolane, 4,4,5,5-tetramethyl-2-(3,4,5-trimethoxyphenyl)-1,3,2-dioxaborolane and 2-(4-methoxy-8-methylnaphthalen-1-yl)-4,4,5,5-tetra-methyl-1,3,2-dioxaborolane have been prepared by reacting the corresponding aryl bromides[SI-1] with bis(pinacolato)diboron according to standard procedures.[SI-2]

3. Preparation of bromonaphthalene dicarboximide 2[SI-3]

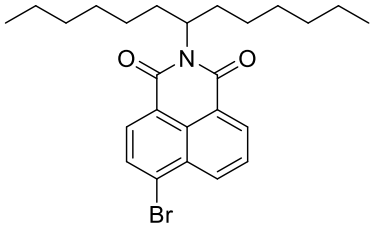

A mixture of tridecan-7-amine (6.60 g, 33.0 mmol, 1.50 equiv) and 4-bromo-1,8-naphthalic anhydride (6.00 g, 22.0 mmol, 1.00 equiv) in ethylene glycol (50 mL) was heated at 160 °C. After 12 h, hydrochloric acid (2 M, 50 mL) was added to the reaction mixture, which was subsequently extracted with $CHCl_3$ (3 x 50 mL). The combined organic phases were dried over $MgSO_4$ and concentrated *in vacuo*. Column chromatography ($CHCl_3$) gave **2** as yellow oil (9.05 g, 90%).

4. Analysis of the solvatochromism of naphthalimides 3

4.1. Analysis of the solvatochromism of compounds 3 according to Kawski's method

The solvatochromism of the series of **3** was analysed with the method reported by Kawski and coworkers.[12,SI-4] There, the function f_{BK} was established by means of equation (SI-1) and the function g_{BK} by means of equation (SI-2), respectively, where n is the index of refraction of the solvent and ε the relative permittivity.

$$f_{BK} = \frac{2n^2+1}{n^2+2}\left(\frac{\varepsilon-1}{\varepsilon+2} - \frac{n^2-1}{n^2+2}\right) \quad \text{(SI-1)}$$

$$g_{BK} = \frac{3}{2}\frac{n^4-1}{(n^2+2)^2} \quad \text{(SI-2)}$$

Characteristic indicators for solvent effects are m_1 obtained as the slope of a linear plot of the Stokes' shift ν_{abs}-ν_{flu} (in kK as wavenumbers 1000 cm^{-1}) versus f_{BK} and m_2 as the slope of the sum of the wavenumbers of the maxima of UV/Vis absorption and fluorescence ν_{abs}+ν_{flu} versus f_{BK}+2g_{BK} and are reported in Table SI-1.

Table SI-1. Slopes m_1 and m_2 and correlation numbers $r_{(m1)}$ and $r_{(m2)}$ (6 solvents except **3c** with 5 solvents; solvents: 1-Butanol, 1-undecanol, *N*,*N*-dimethylformamide, toluene (except for **3h**), *n*-hexane, *n*-tetradecane. μ_e/μ_g: Calculated ratio of dipole moments in electronically excited μ_e and the ground state μ_g. according to equation (SI-3).

Nr.	m_1 kK	$r_{(m1)}$	m_2 kK	$r_{(m2)}$	μ_e/μ_g
3a	0.51	0.917	-3.00	-0.976	1.4
3b	3.06	0.989	-5.11	-0.979	4.0
3c	5.24	0.928	-10.21	-0.959	3.1
3d	5.89	0.960	-7.56	-0.978	8.0
3g	6.69	0.956	-7.21	-0.975	26.7
3h	6.32	0.957	-6.93	-0.977	21.7
3i	0.69	0.911	-2.94	-0.930	1.6
3j	3.24	0.989	-5.29	-0.975	4.2
3l	5.80	0.998	-8.01	-0.992	6.2

$$\frac{\mu_e}{\mu_g} = \frac{|m_1| + |m_2|}{|m_2| - |m_1|} \qquad \text{(SI-3)}$$

The ratio μ_e/μ_g according to equation (SI-3) indicates the alteration of the dipole moment in the electronically excited state μ_e and the ground state μ_g for parallel transition moments. We applied μ_e/μ_g according to equation (SI-3) as a scale for the solvent influence on the electronic spectra. A clear maximum was found for the preferred **3g** verifying the concept of twisted donor acceptor systems for strong solvatochromism. This exceeds even the effect of the prolonged electronic system in **3l**.

The linear correlations on the basis of f_{BK} and g_{BK} are reported in the subsequent Fig. SI-1 to SI-9.

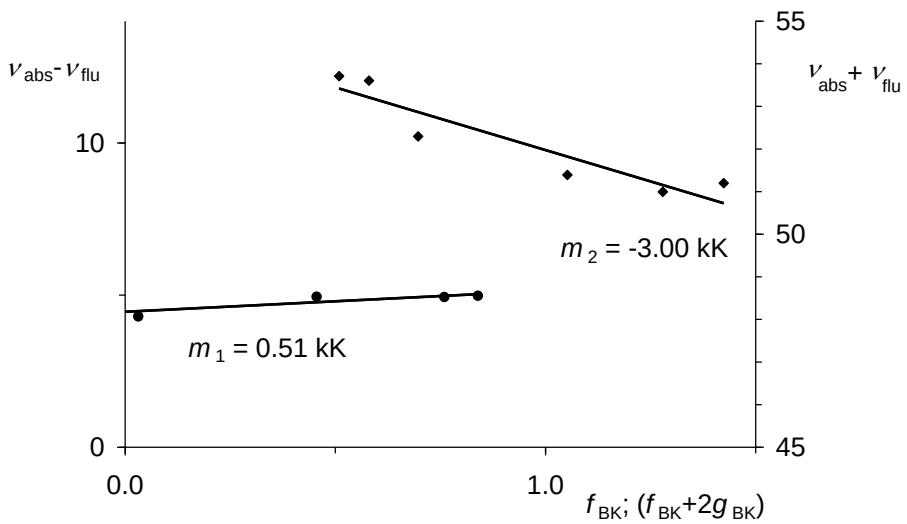

Fig. SI-1. Linear correlations of the Stokes' shift ν_{abs}-ν_{flu} (in 1000 cm^{-1}) of **3a** versus f_{BK} to obtain m_1 and of the sum ν_{abs}+ν_{flu} versus f_{BK}+2g_{BK} to obtain m_2.

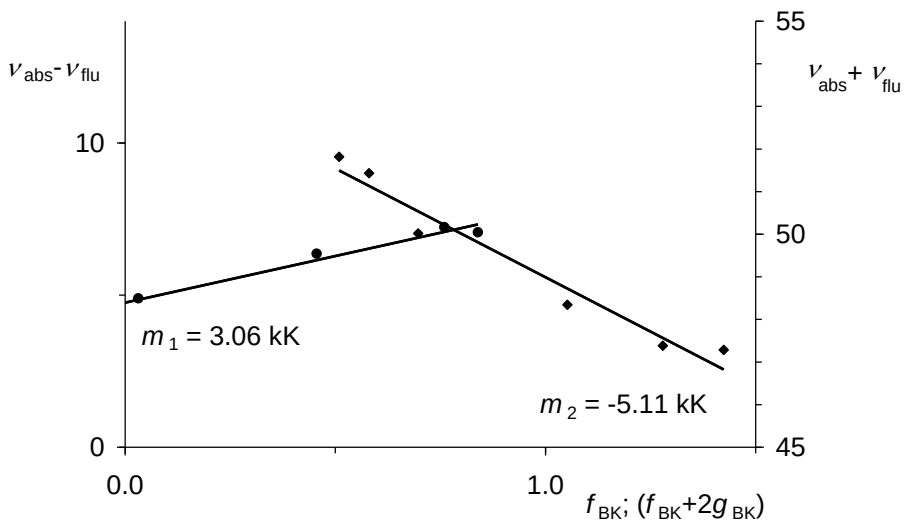

Fig. SI-2. Linear correlations of the Stokes' shift ν_{abs}-ν_{flu} (in 1000 cm^{-1}) of **3b** versus f_{BK} to obtain m_1 and of the sum ν_{abs}+ν_{flu} versus f_{BK}+2g_{BK} to obtain m_2.

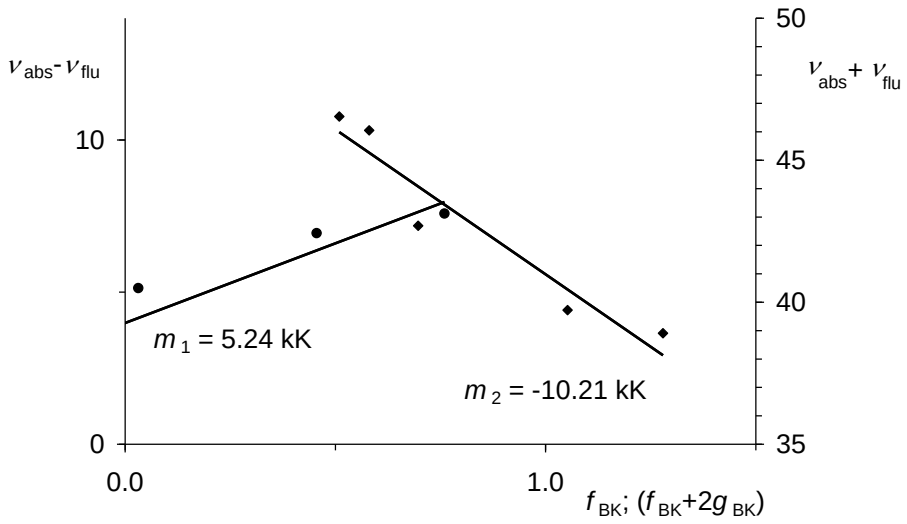

Fig. SI-3. Linear correlations of the Stokes' shift ν_{abs}-ν_{flu} (in 1000 cm^{-1}) of **3c** versus f_{BK} to obtain m_1 and of the sum ν_{abs}+ν_{flu} versus f_{BK}+2g_{BK} to obtain m_2.

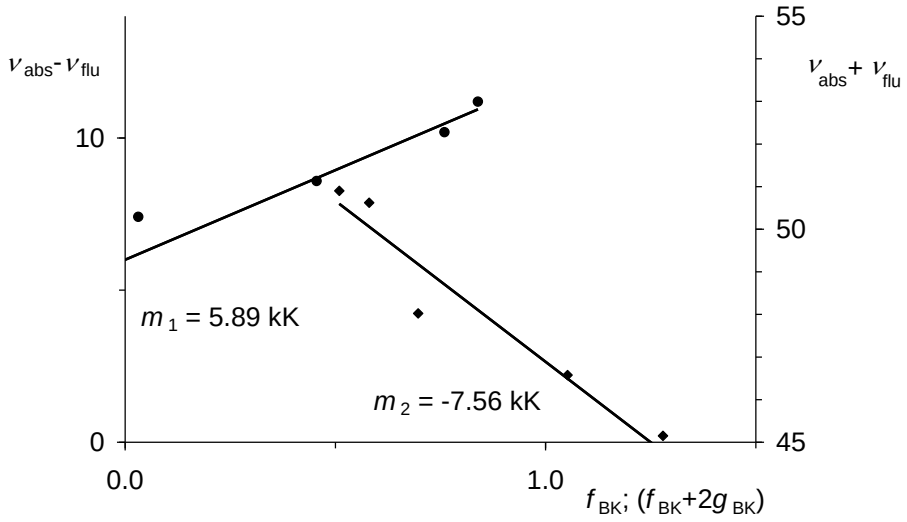

Fig. SI-4. Linear correlations of the Stokes' shift ν_{abs}-ν_{flu} (in 1000 cm^{-1}) of **3d** versus f_{BK} to obtain m_1 and of the sum ν_{abs}+ν_{flu} versus f_{BK}+2g_{BK} to obtain m_2.

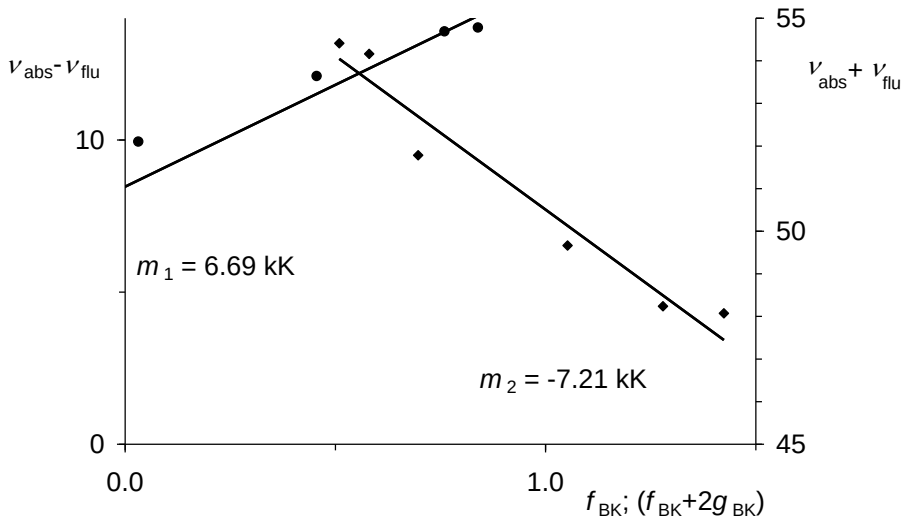

Fig. SI-5. Linear correlations of the Stokes' shift ν_{abs}-ν_{flu} (in 1000 cm^{-1}) of **3g** versus f_{BK} to obtain m_1 and of the sum ν_{abs}+ν_{flu} versus f_{BK}+2g_{BK} to obtain m_2.

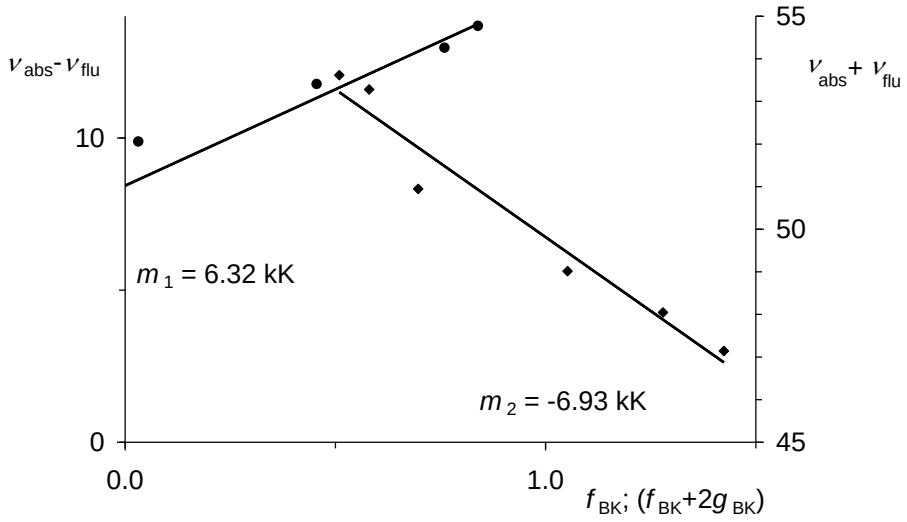

Fig. SI-6. Linear correlations of the Stokes' shift ν_{abs}-ν_{flu} (in 1000 cm^{-1}) of **3h** versus f_{BK} to obtain m_1 and of the sum ν_{abs}+ν_{flu} versus f_{BK}+2g_{BK} to obtain m_2.

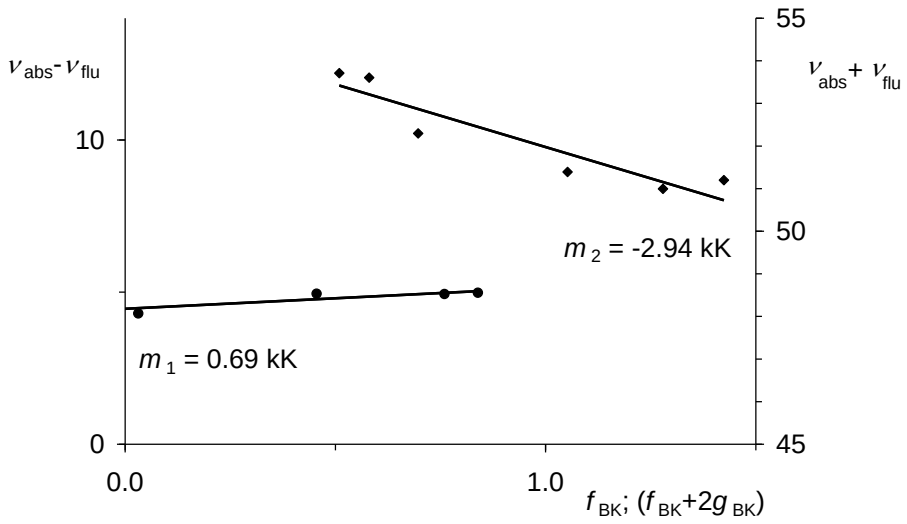

Fig. SI-7. Linear correlations of the Stokes' shift ν_{abs}-ν_{flu} (in 1000 cm^{-1}) of **3i** versus f_{BK} to obtain m_1 and of the sum ν_{abs}+ν_{flu} versus f_{BK}+2g_{BK} to obtain m_2.

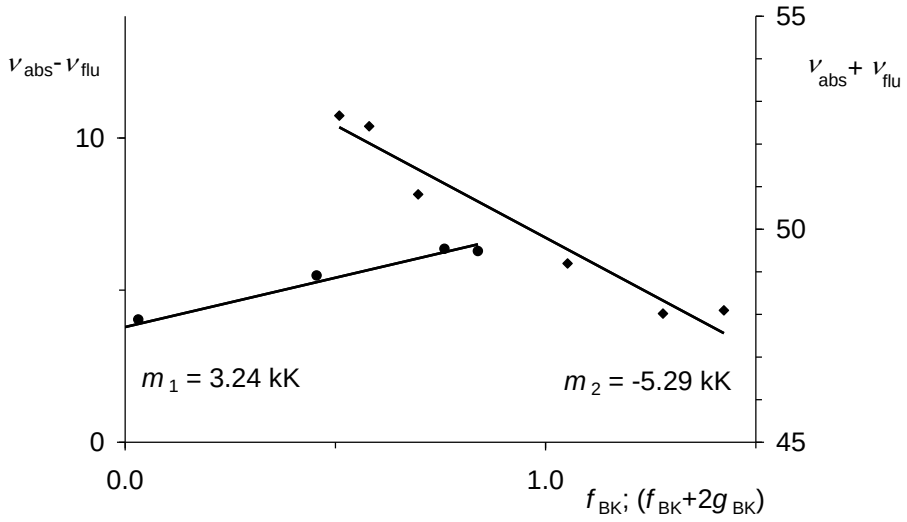

Fig. SI-8. Linear correlations of the Stokes' shift ν_{abs}-ν_{flu} (in 1000 cm^{-1}) of **3j** versus f_{BK} to obtain m_1 and of the sum ν_{abs}+ν_{flu} versus f_{BK}+2g_{BK} to obtain m_2.

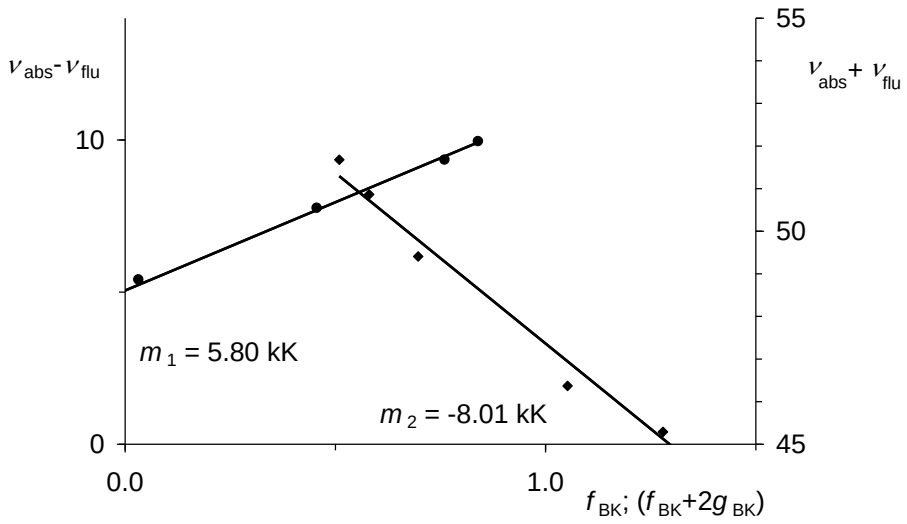

Fig. SI-9. Linear correlations of the Stokes' shift ν_{abs}-ν_{flu} (in 1000 cm^{-1}) of **3l** versus f_{BK} to obtain m_1 and of the sum ν_{abs}+ν_{flu} versus f_{BK}+2g_{BK} to obtain m_2.

4.2. Analysis of solvatochromism of compounds 3 by means of the multi parameter approach of Kamlet, Taft and Abboud

The solvatochromism of the series of **3** was analysed by means of the multi parameter approach of equation (1) developed by Kamlet, Taft and Abboud[13,SI-5] where solvent effects were generalized to any solvent-dependent property *XYZ*. The sensitivity to dipolar-polarizability term is characterized by *s* where a correction *d* concerns the polarizability. The paramers *a* and *b* are attributed to hydrogen acceptor and donor properties. We applied equation (SI-4) to the E_T values of the fluorescence (E_T=28591 kcal·nm/λ_{max}) of the series of **3**, obtained equation (SI-5) and optimized the parameters of equation (SI-5) by least square-fitting. The results are reported in Table SI-2 where the values *s* indicates a generally pronounced sensitivity of **3** to solvent effects. Large *s*-values were found for the favoured **3g**, but also for **3d**, **3h** and **3l**. A minor variation is found for the parameter *d* except for the dimethylaminophenyl derivative **3c**. A high value of *a* is found for the latter as one my expect for acceptors of hydrogen bonds. There are only minor variations for the other values of *a* and *b* in accordance with the lack of pronounced effects of hydrogen bonds.

$$XYZ = XYZ_0 + s\,(\pi^* + d\delta) + a\alpha + b\beta \quad \text{(SI-4)}$$

$$E_T = XYZ_0 + s\,(\pi^* + d\delta) + a\alpha + b\beta \quad \text{(SI-5)}$$

Table SI-2. Calculated parameters XYZ_0, *s*, *d*, *a* and *b* by means of least square fits of the experimental E_T values of fluorescence of **3** according to equation (SI-5). Solvents: 1-Butanol, *N*,*N*-dimethylformamide, chloroform, toluene, *n*-hexane.

Nr.	XYZ_0	*s*	*d*	*a*	*b*
3a	70.71	-3.64	-0.27	-2.30	-0.83
3b	66.85	-7.32	-0.28	-3.25	-4.20
3c	61.29	-6.29	0.60	-14.37	-3.80
3d	63.62	-16.68	-0.23	-3.26	-3.95
3g	65.80	-14.22	-0.17	-6.00	-6.02
3h	64.48	-15.94	-0.20	-4.92	-3.80
3i	70.00	-3.75	-0.20	-2.24	-0.91
3j	69.51	-8.41	-0.27	-4.25	-3.38
3l	65.77	-15.18	-0.39	-4.12	-4.94

4.3. Analysis of solvatochromism of compounds 3 by means of the multi parameter approach of Catalán

The multi parameter approach of equation (SI-6) of Catalán[14,SI-6] with the generalized solvent effect *A* was applied to the E_T-values (E_T=28591 kcal·nm/λ_{max}) of the solvatochromism of fluorescence to obtain equation (SI-7).

$$A = A_0 + b\mathrm{SA} + c\mathrm{SB} + d\mathrm{SP} + e\mathrm{SdP} \quad \text{(SI-6)}$$

$$E_T = A_0 + b\mathrm{SA} + c\mathrm{SB} + d\mathrm{SP} + e\mathrm{SdP} \quad \text{(SI-7)}$$

We applied equation (SI-7) to the fluorescence of the series of **3** and optimized the parameters A_0, *b*, *c*, *d* and *e* by means of least square fitting; see Table 1.

Table SI-3. Optimized parameters A_0, *b*, *c*, *d* and *e* of equation (SI-7) by means of least square fitting of the experimental E_T-values of the fluorescence of **3** in the solvents 1-butanol, 1-undecanol, *N*,*N*-dimethylformamide, chloroform, toluene, *n*-hexane, *n*-tetradecane. (*N*,*N*-Dimethylformamide was excluded for **3c** because of lack of fluorescence). *r*: Correlation number.

Nr.	A_0	*b*	*c*	*d*	*e*	*r*
3a	72.6	-5.53	-0.10	-2.46	-3.72	0.9987
3b	68.7	-6.02	-3.62	-2.07	-7.36	0.9991
3c	72.6	16.33	-13.69	-12.67	-17.60	1.0000
3d	71.6	-2.02	-4.99	-10.11	-14.93	0.9984
3g	77.3	-12.74	-4.77	-16.11	-12.93	0.9989
3h	77.4	-7.30	-5.19	-18.05	-12.80	0.9995
3i	74.5	-5.10	-1.07	-6.41	-2.87	0.9953
3j	72.9	-8.83	-2.43	-4.37	-8.22	0.9998
3l	66.1	-1.74	-7.49	1.15	-13.48	0.9966

The parameter *e* can be applied as a measure of the sensitivity concerning the dipolarity of the solvent SdP where high negative valued were found for the donor- substituted derivatives **3c**, **3d**, **3g**, **3h** and **3l**. The effect of a simple 4-methoxyphenyl group in **3b** is appreciably smaller. The parameter *d* for the solvent polarizability SP is found to be strongly negative for **3c**, **3d**, **3g** and **3h** indicating a boosting solvent effect of dipolarity and polarizability for these compounds. The parameters *b* and *c* concerning solvent acidity SA and solvent basicity SB are not pronounced except of *b* for **3c** because of the hydrogen-bonding ability of the dimetylamino group. The *b*-value for **3g** is remarkably strong negative indicating a further co-operative solvent effect. As a consequence, compound **3g** can be estimated to be a good compromise concerning solvent effects.

5. NMR-spectra

6-Phenyl-2-(tridecan-7-yl)-1*H*-benzo[*de*]isoquinoline-1,3(2*H*)-dione (3a)

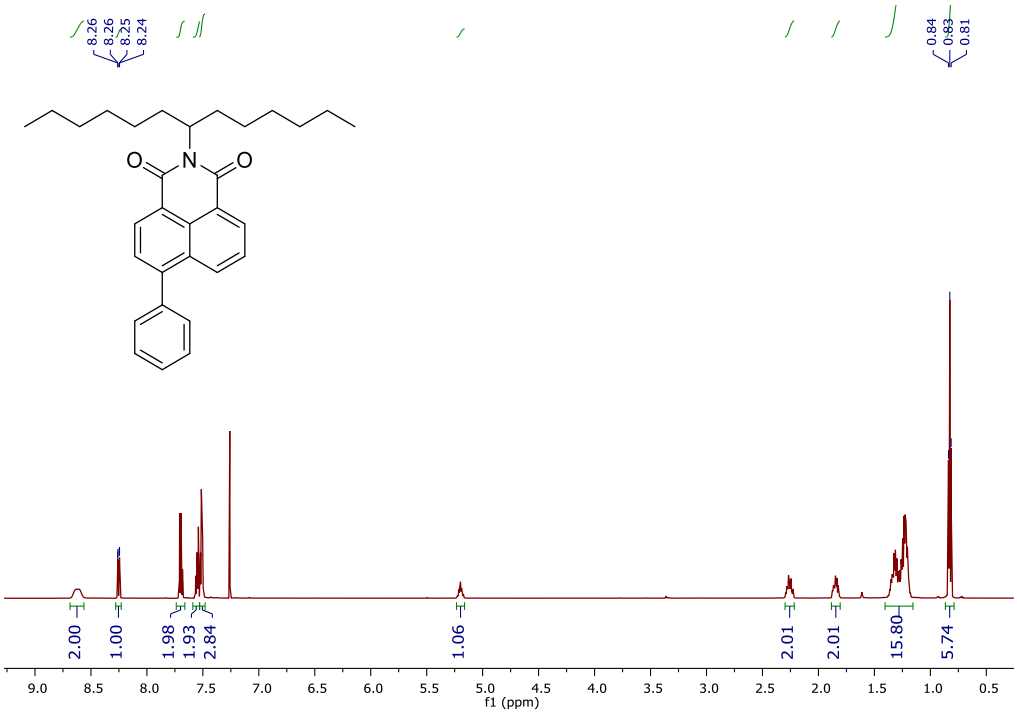

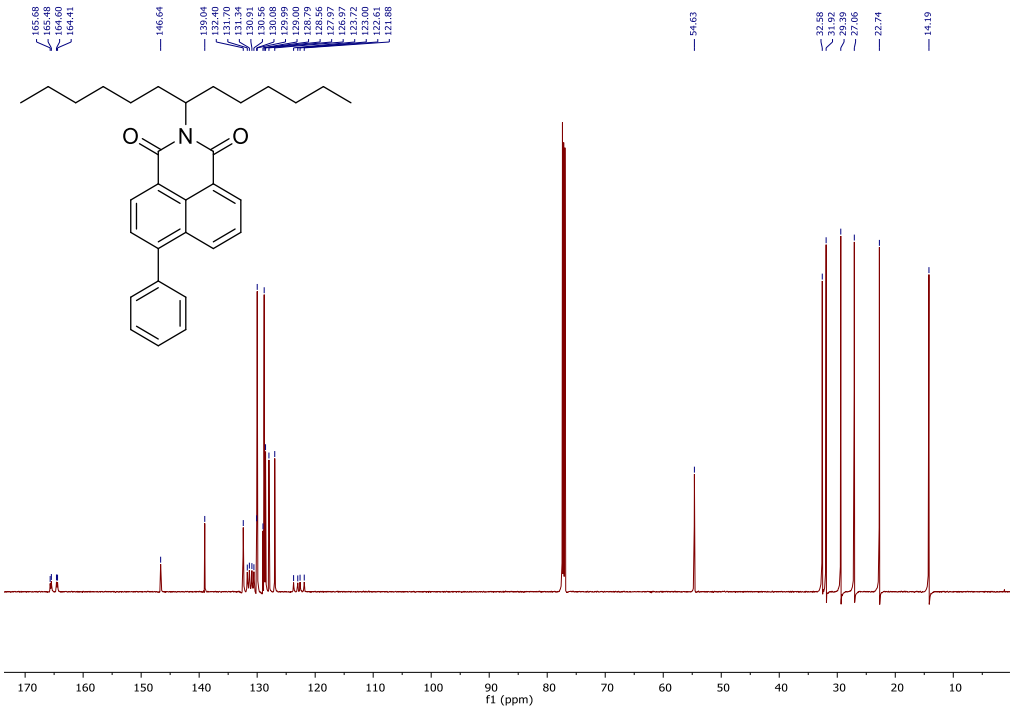

6-(4-Methoxyphenyl)-2-(tridecan-7-yl)-1*H*-benzo[*de*]isoquinoline-1,3(2*H*)-dione (3b)

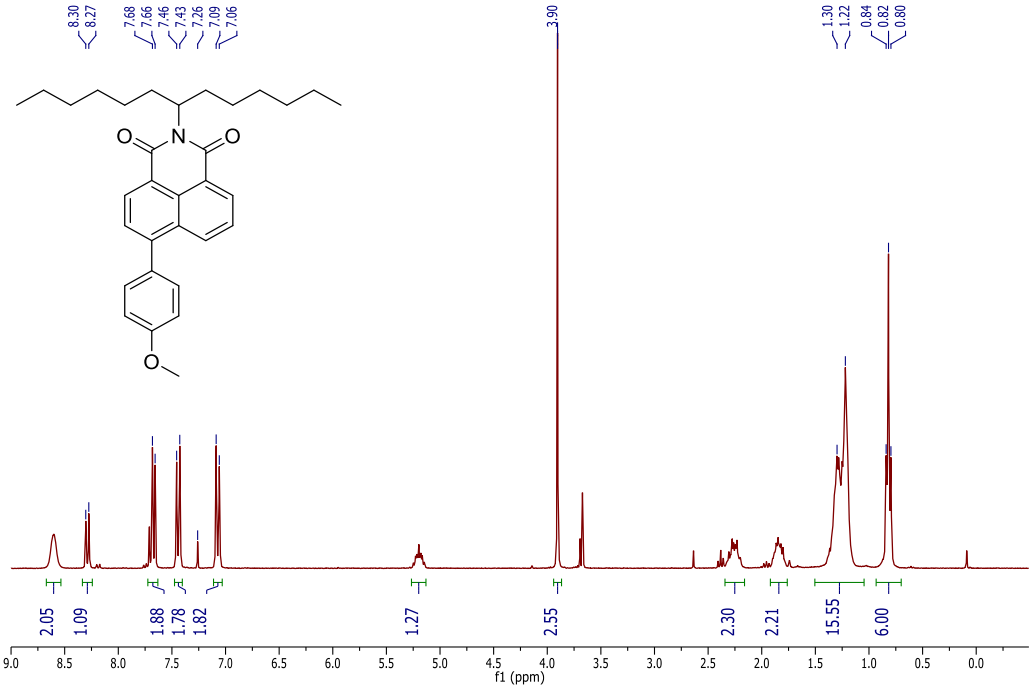

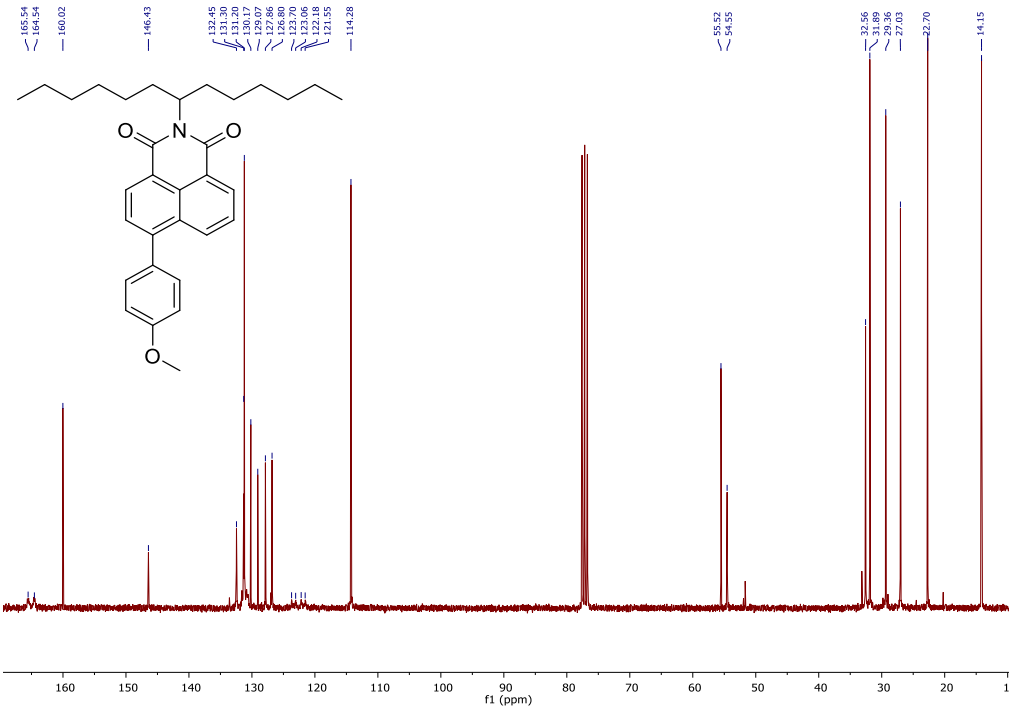

6-(4-(Dimethylamino)phenyl)-2-(tridecan-7-yl)-1*H*-benzo[*de*]isoquinoline-1,3(2*H*)-dione (3c)

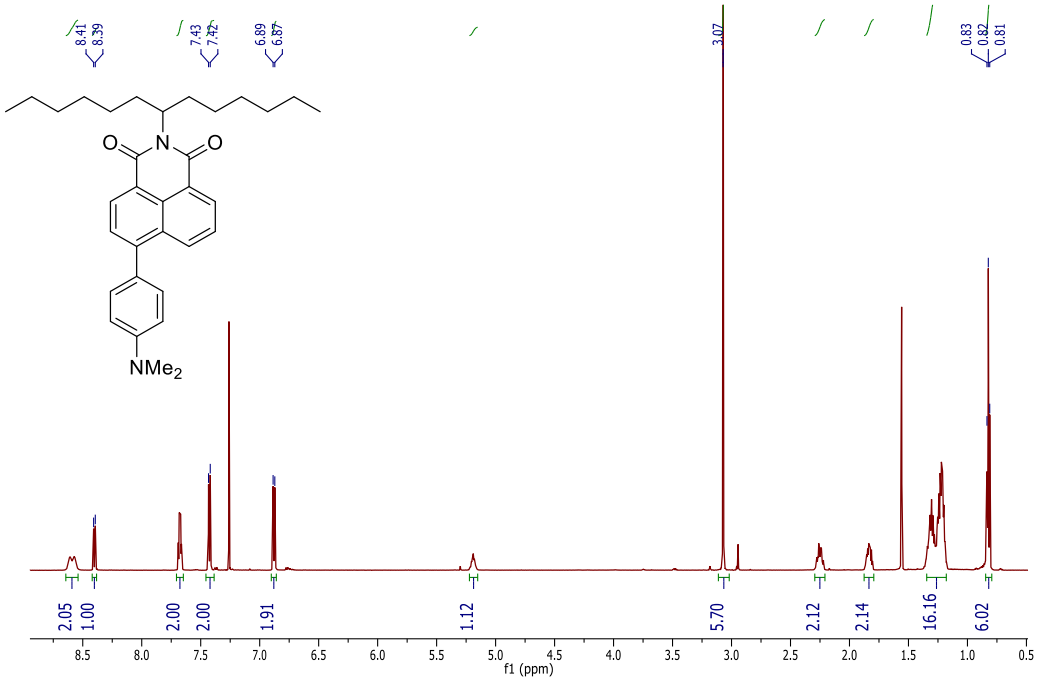

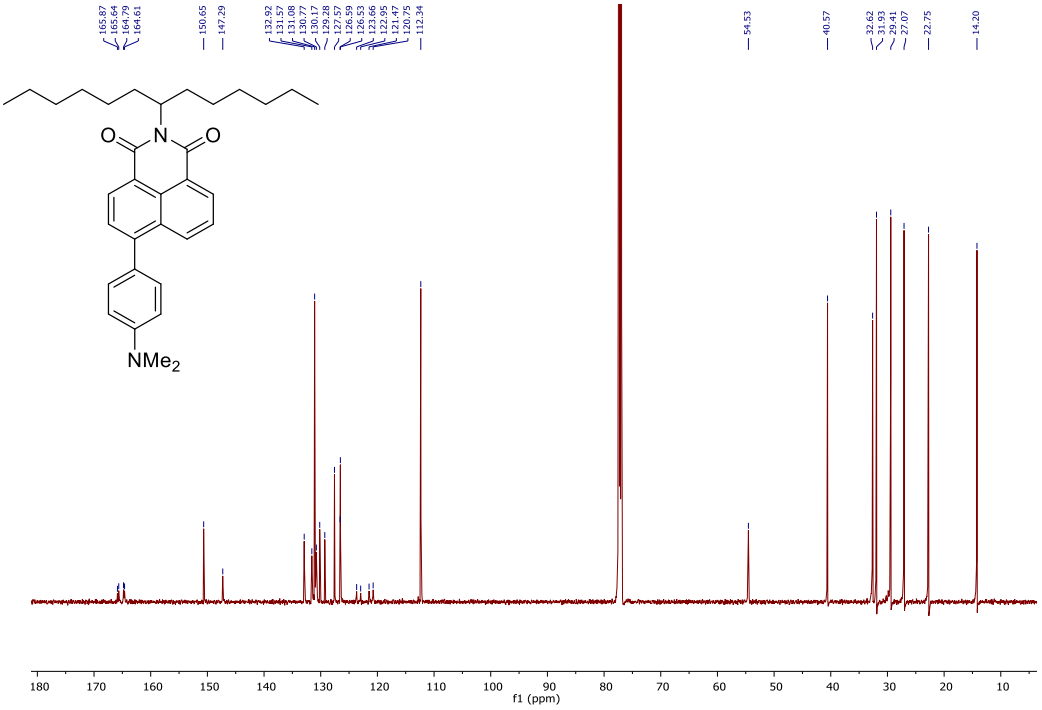

6-(3,4,5-Trimethoxyphenyl)-2-(tridecan-7-yl)-1*H*-benzo[*de*]isoquinoline-1,3(2*H*)-dione (3d)

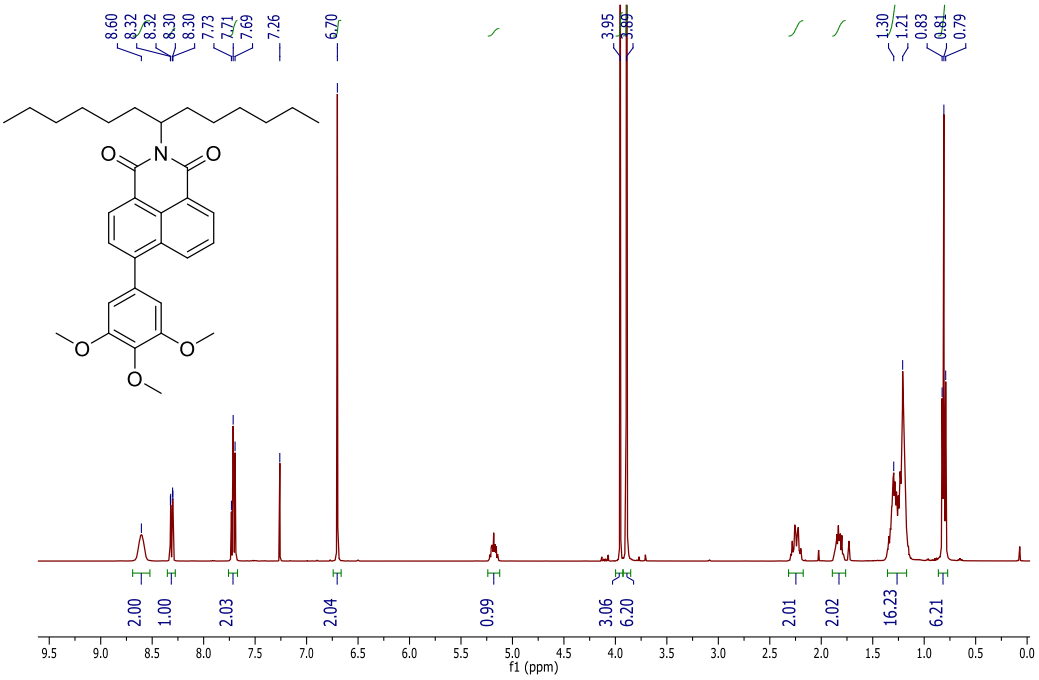

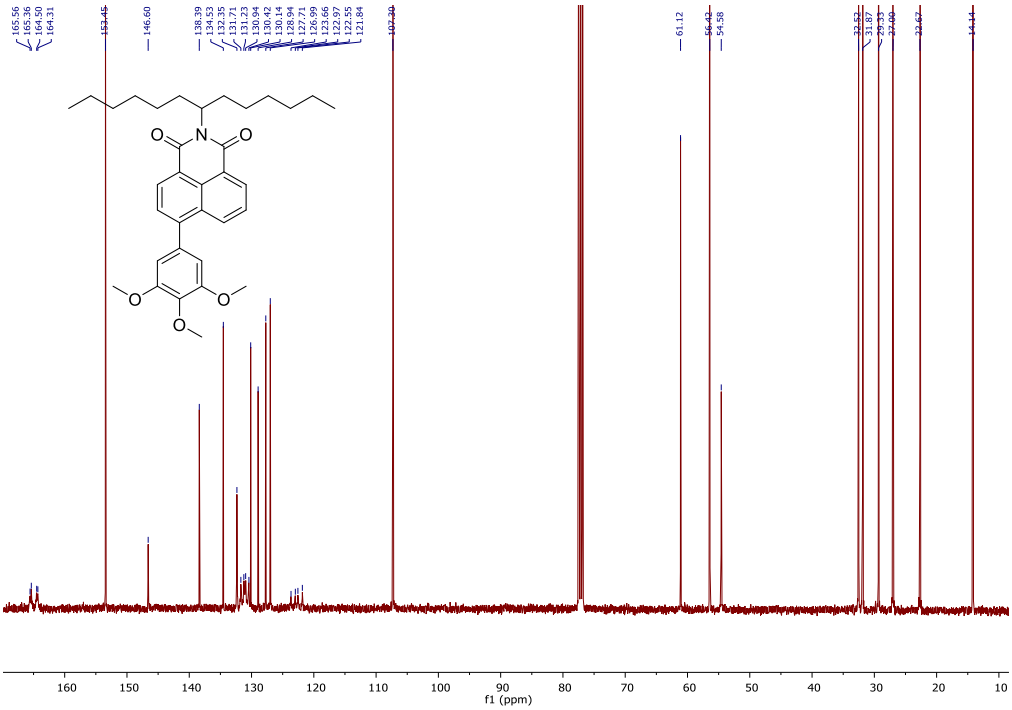

6-(2,6-Dibromo-3,4,5-trimethoxyphenyl)-2-(tridecan-7-yl)-1*H*-benzo[*de*]isoquinoline-1,3(2*H*)-dione (3e)

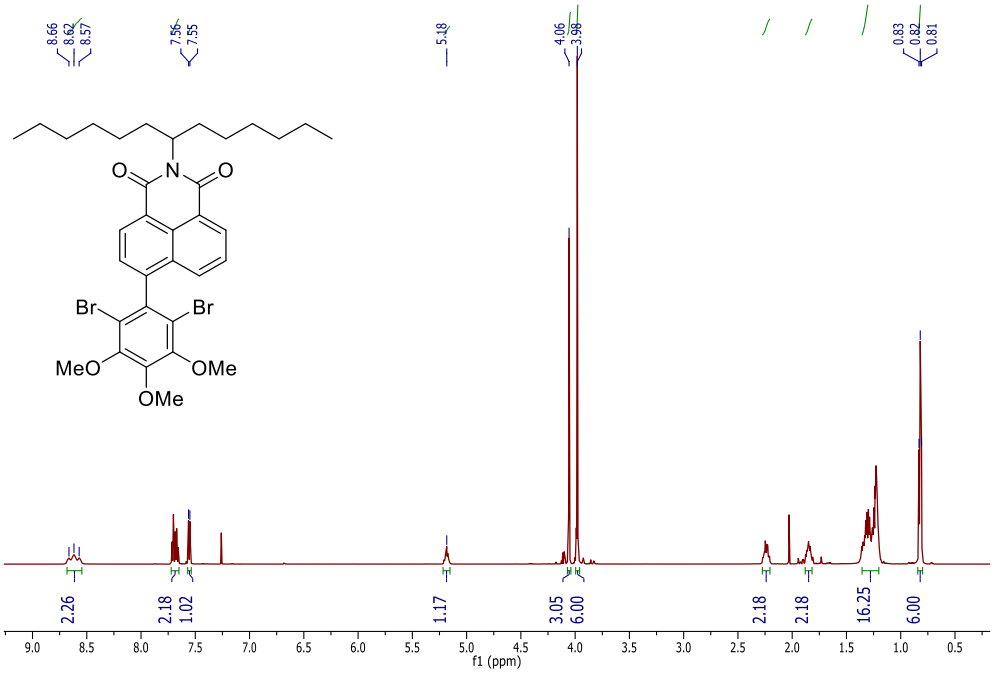

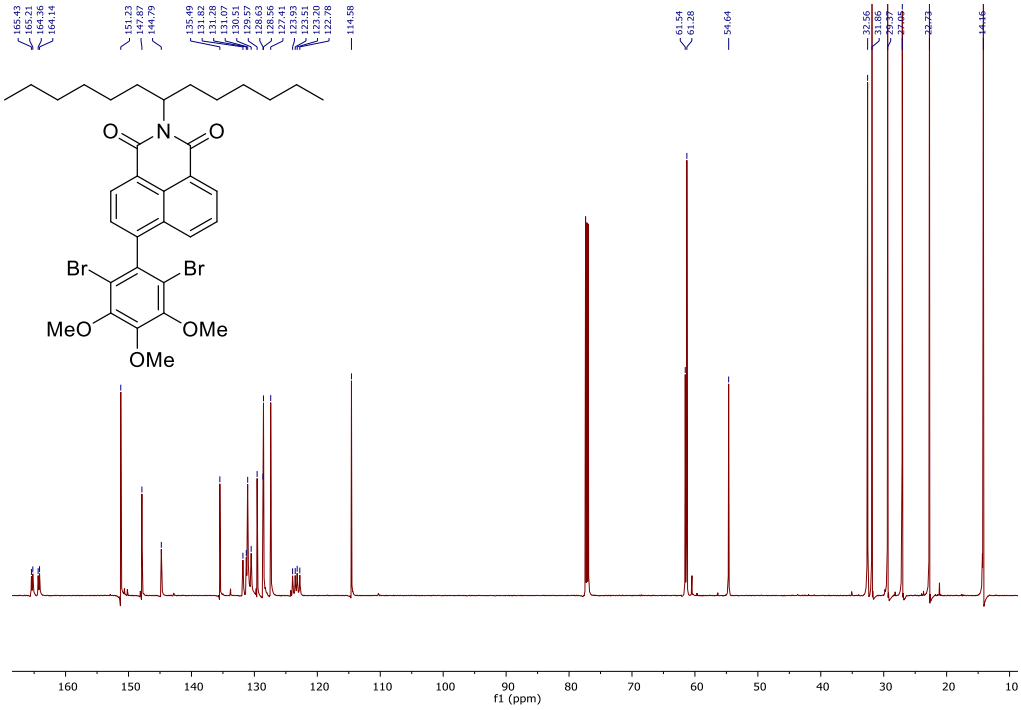

6-(3,4,5-Trimethoxy-2,6-dimethylphenyl)-2-(tridecan-7-yl)-1*H*-benzo[*de*]isoquinoline-1,3(2*H*)-dione (3f)

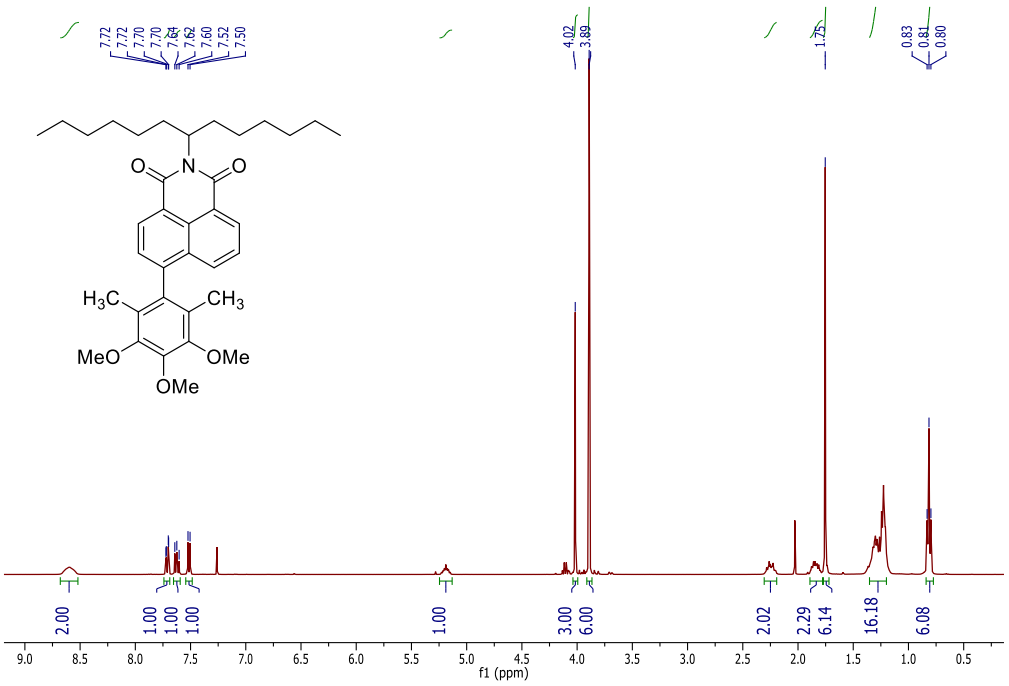

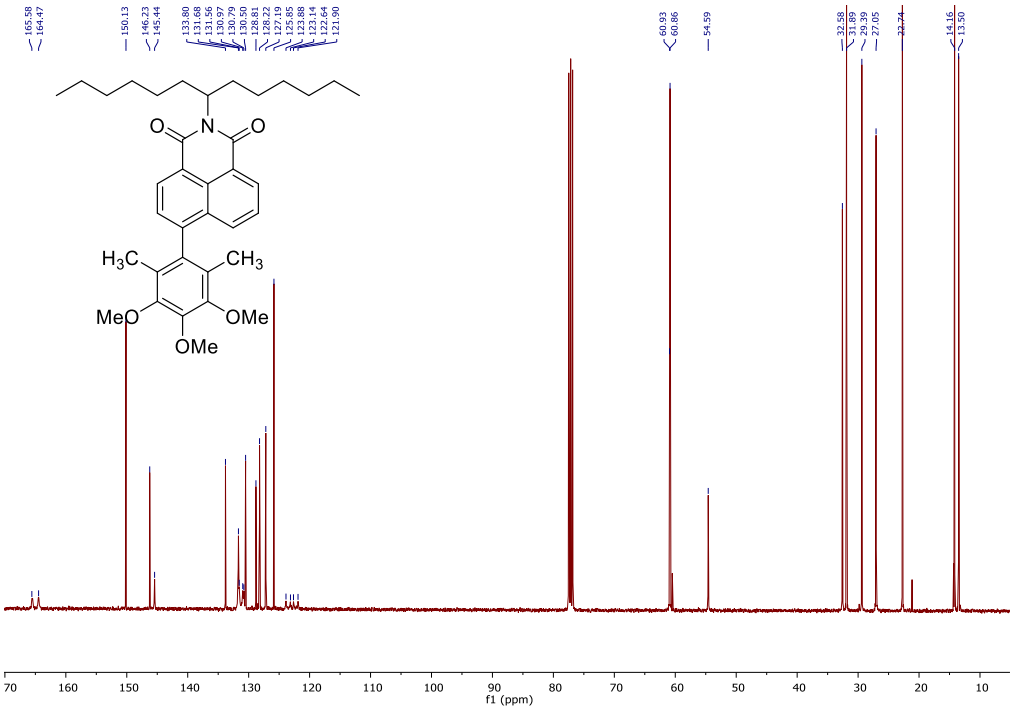

6-(4-Methoxynaphthalen-1-yl)-2-(tridecan-7-yl)-1*H*-benzo[*de*]isoquinoline-1,3(2*H*)-dione (3g)

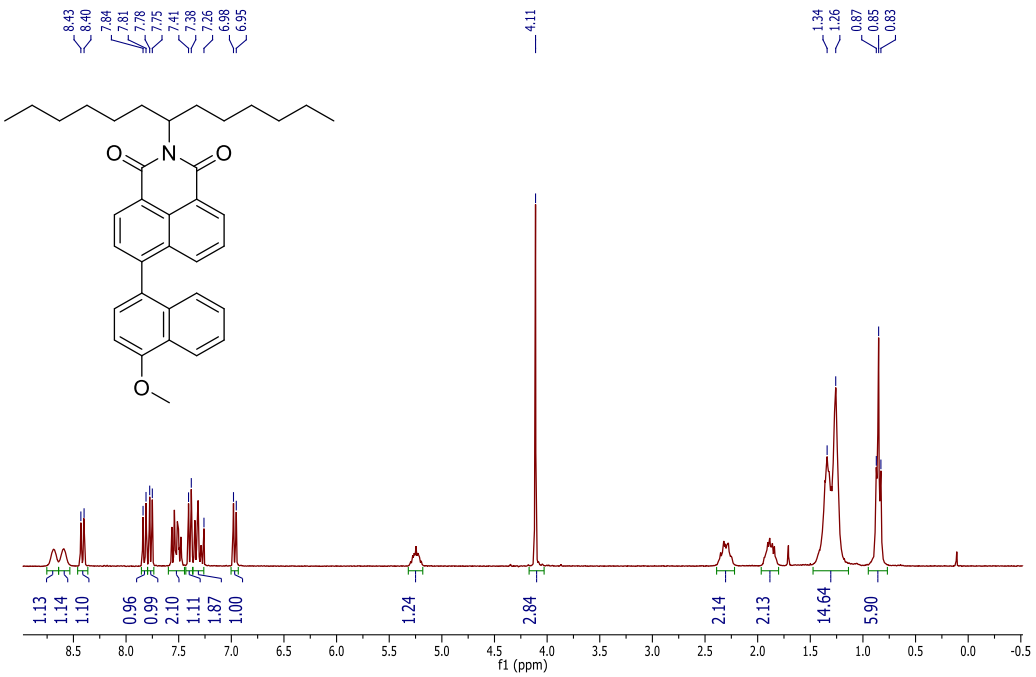

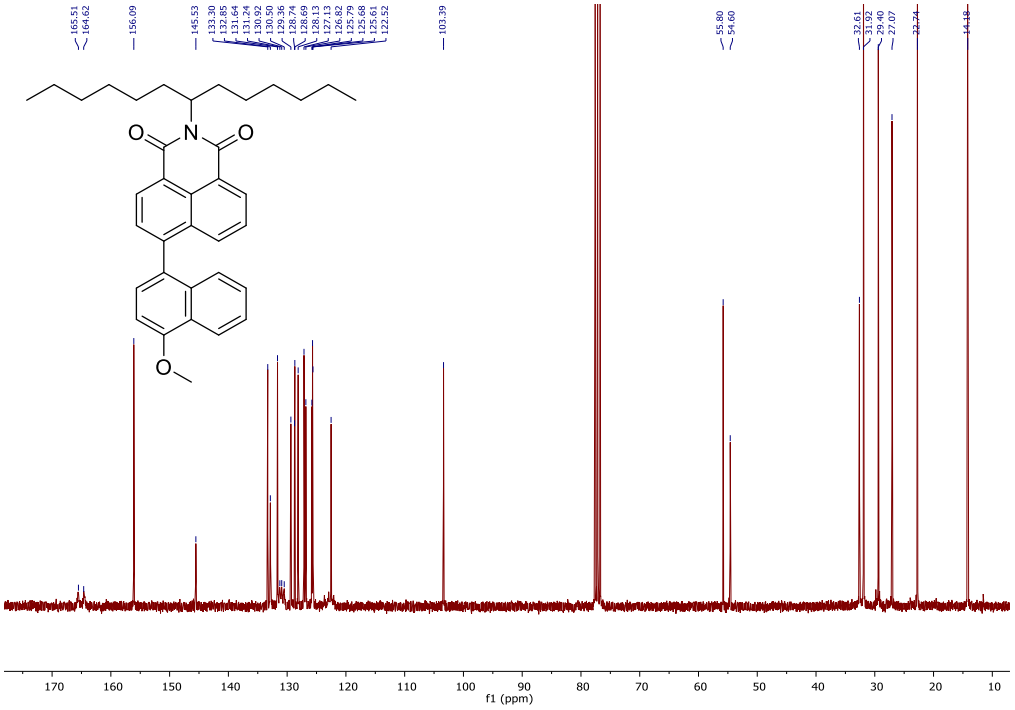

6-(4-Methoxy-8-methylnaphthalen-1-yl)-2-(tridecan-7-yl)-1*H*-benzo[*de*]isoquinoline-1,3(2*H*)-dione (3h)

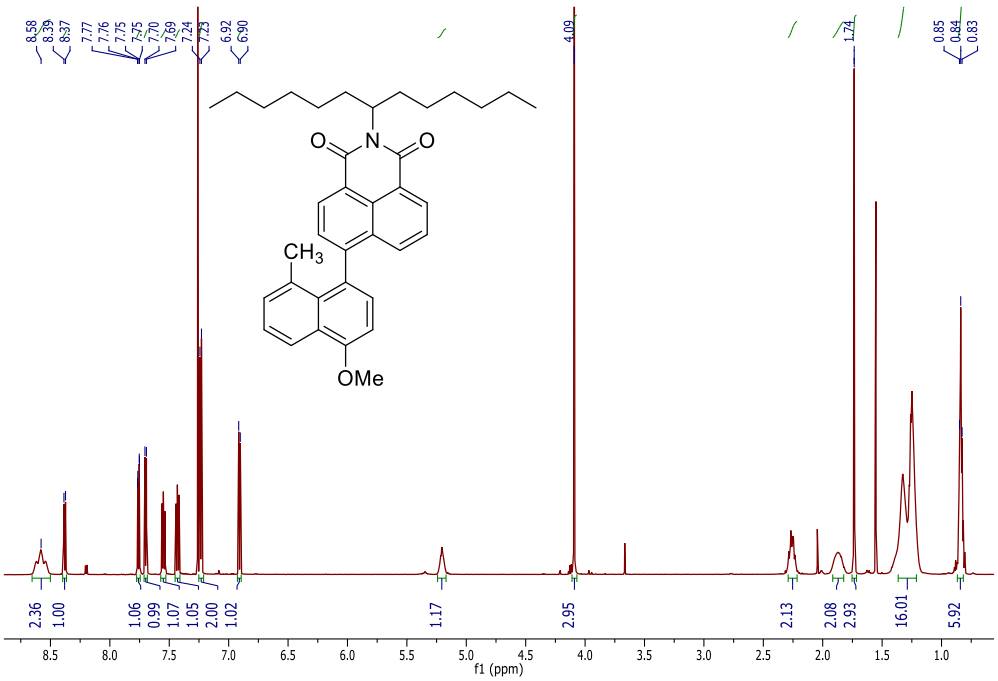

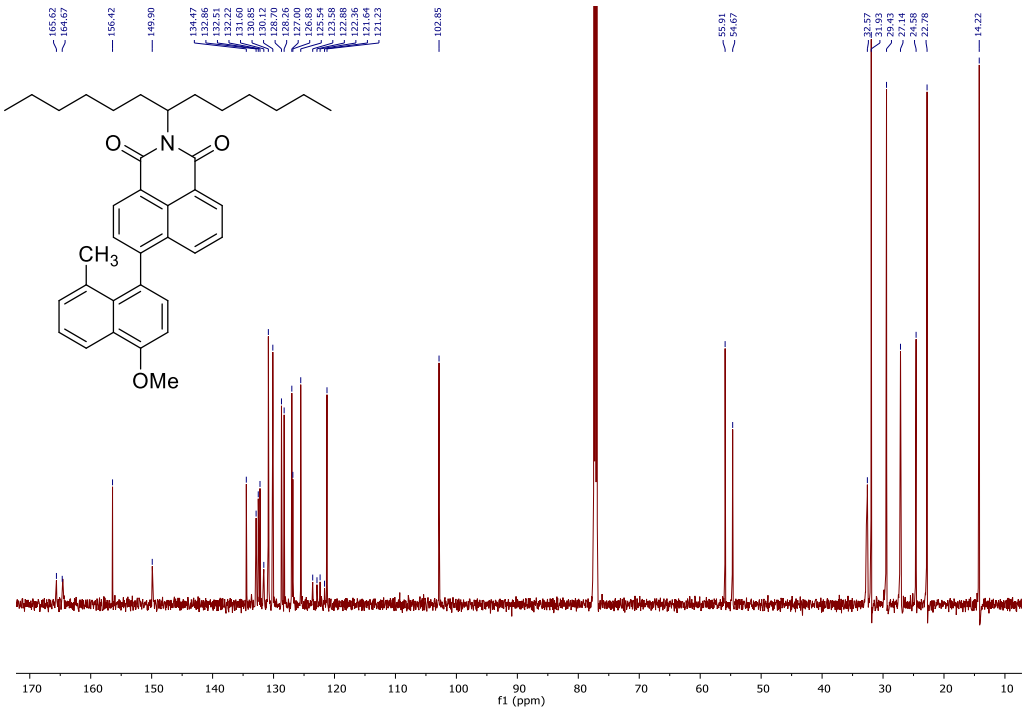

6-(4-(Trimethylsilyl)phenyl)-2-(tridecan-7-yl)-1*H*-benzo[*de*]isoquinoline-1,3(2*H*)-dione (3i)

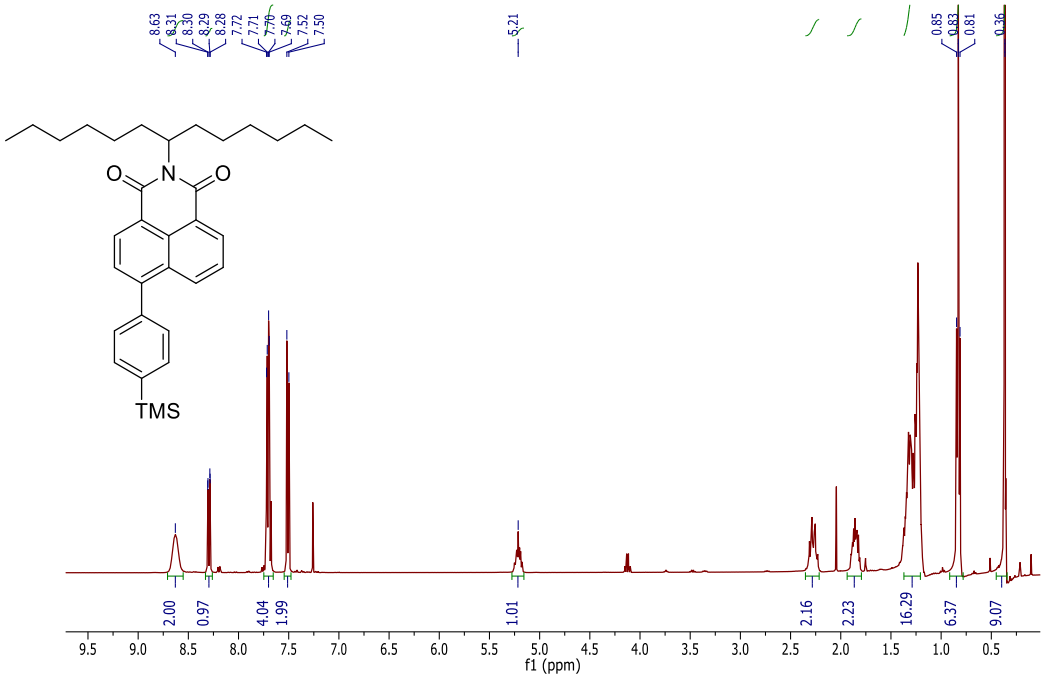

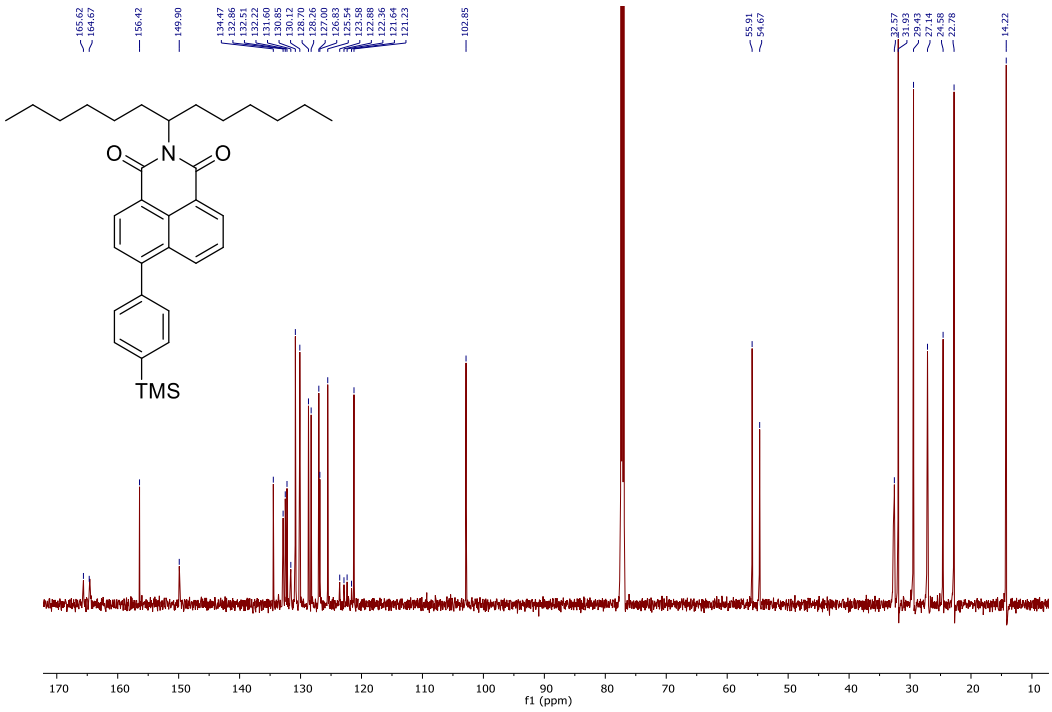

6-(4-Cyanophenyl)-2-(tridecan-7-yl)-1-benzo[*de*]isoquinoline-1,3(2*H*)-dione (3j)

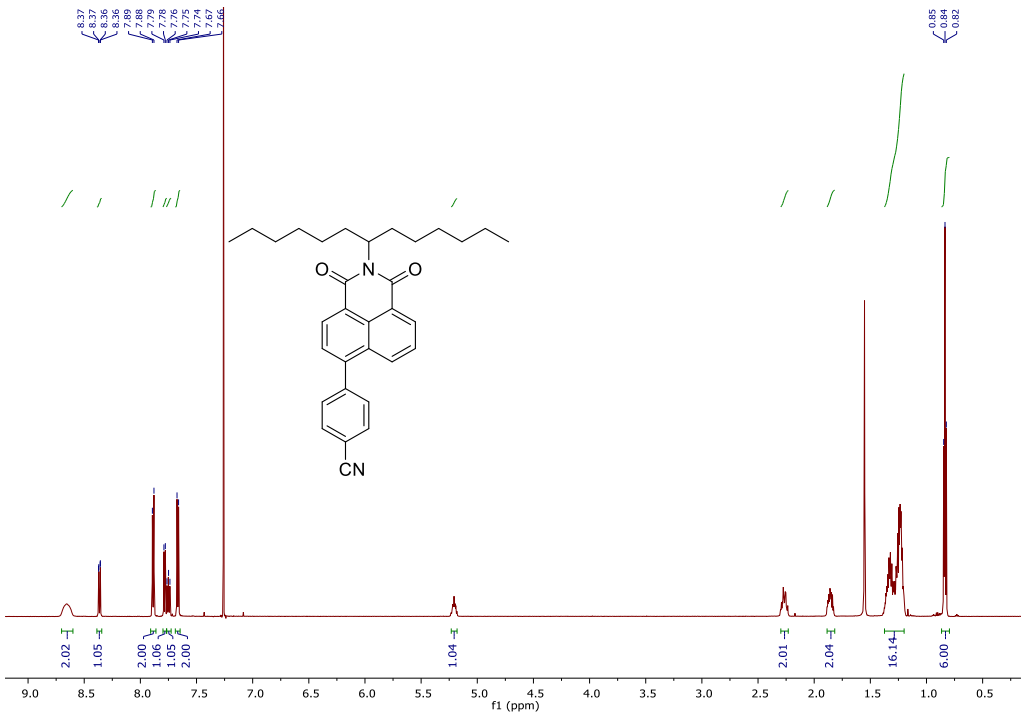

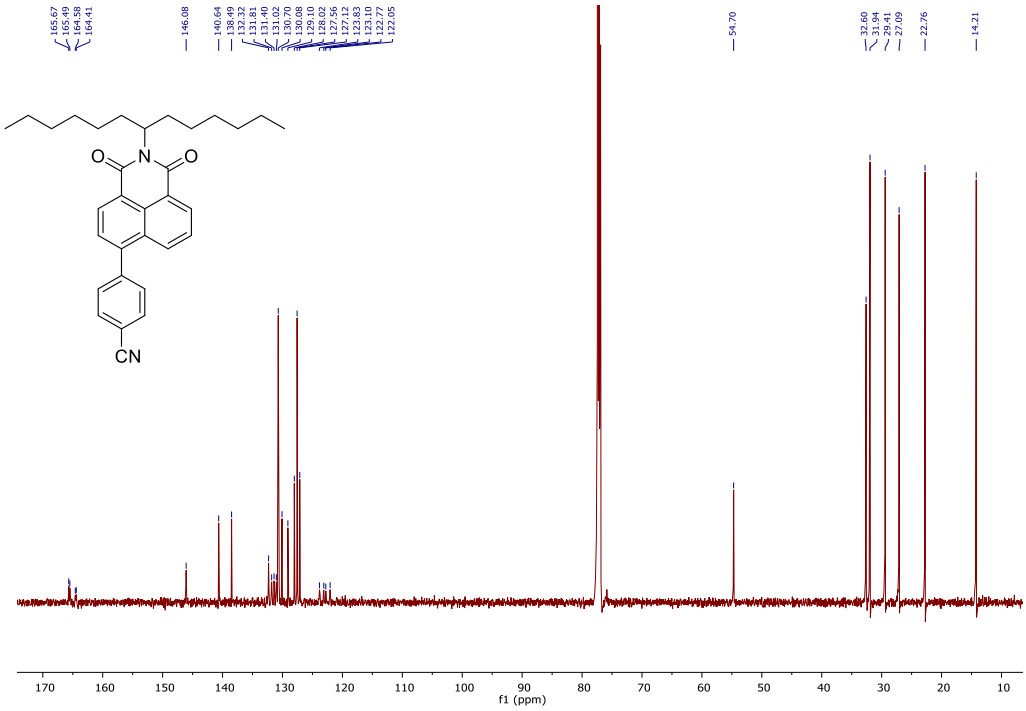

6-(4-Iodophenyl)-2-(tridecan-7-yl)-1*H*-benzo[*de*]isoquinoline-1,3(2*H*)-dione (3k)

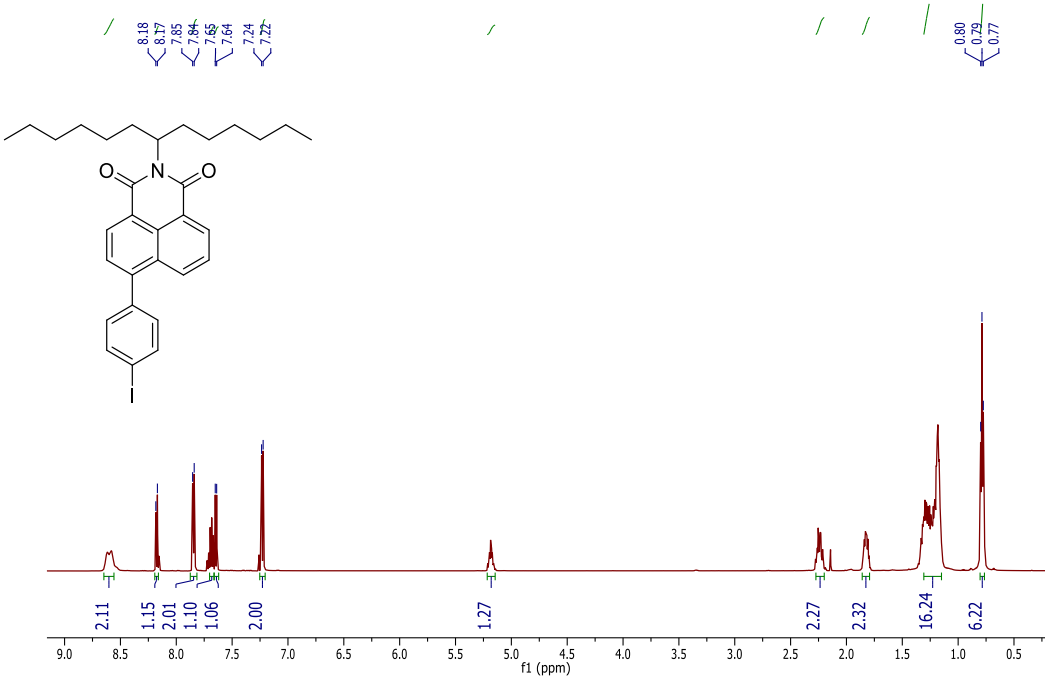

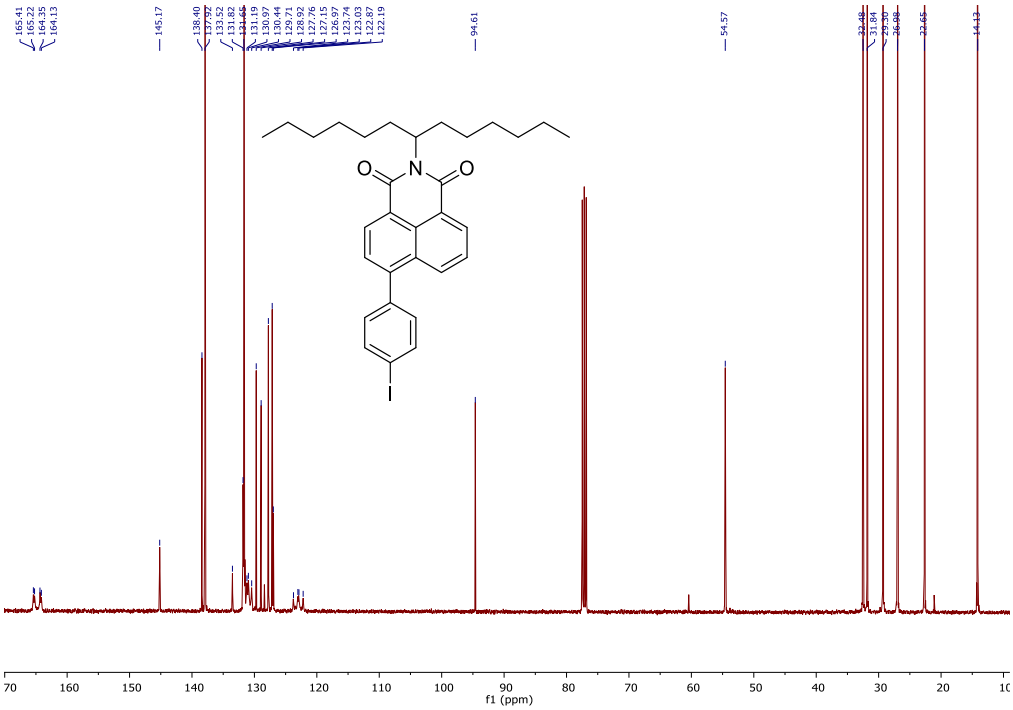

6-(4'-Methoxy-[1,1'-biphenyl]-4-yl)-2-(tridecan-7-yl)-1*H*-benzo[*de*]isoquinoline-1,3(2*H*)-dione (3l)

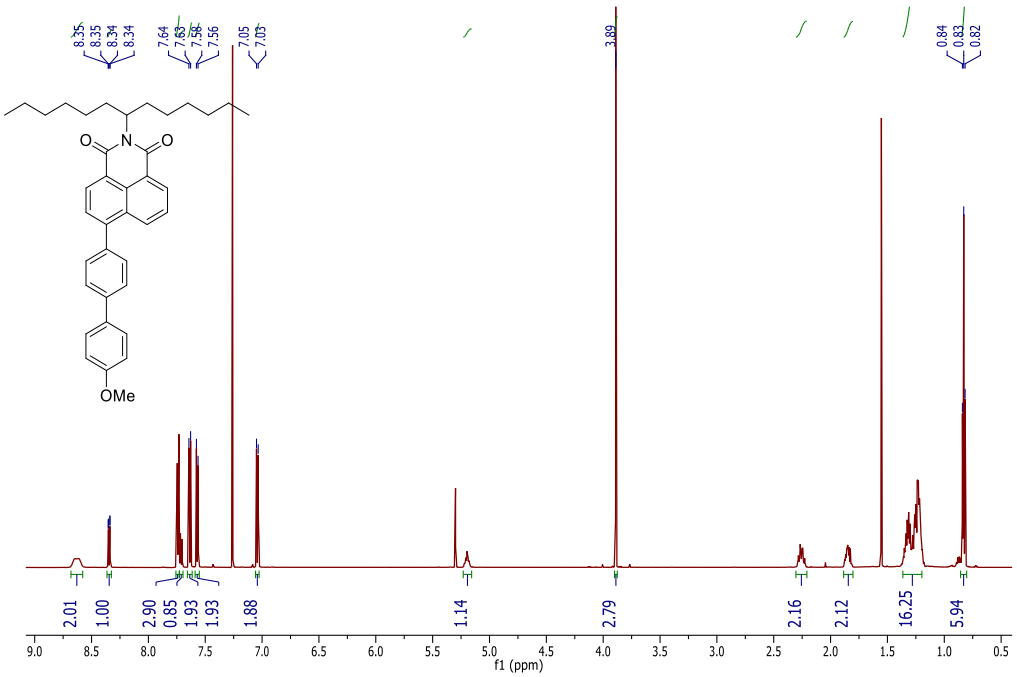

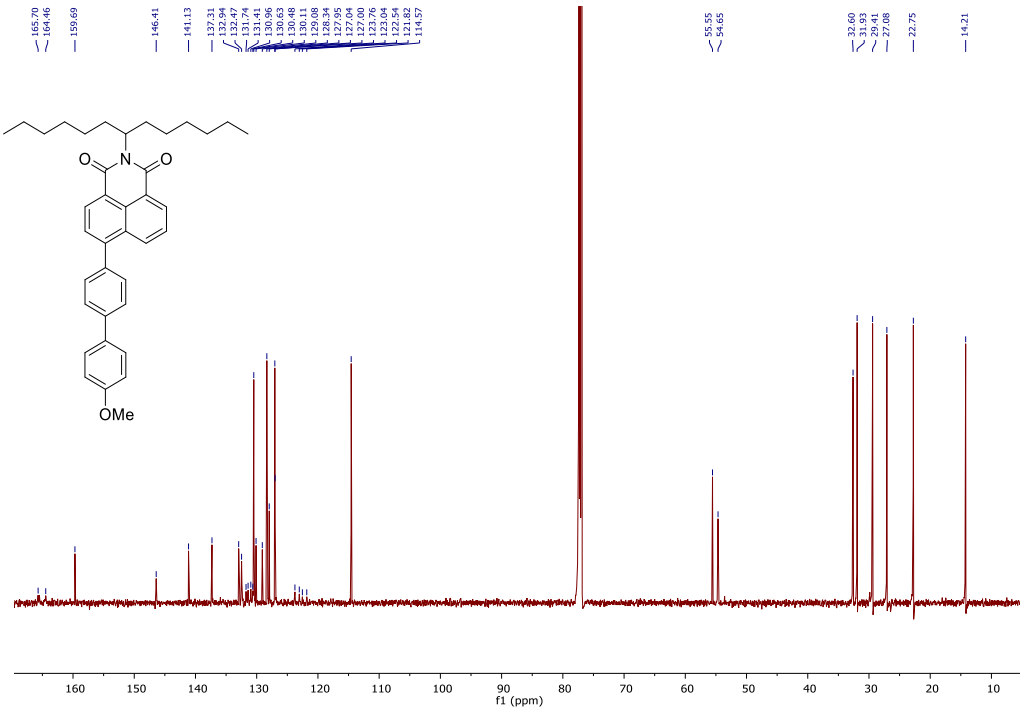

6. IR-spectra

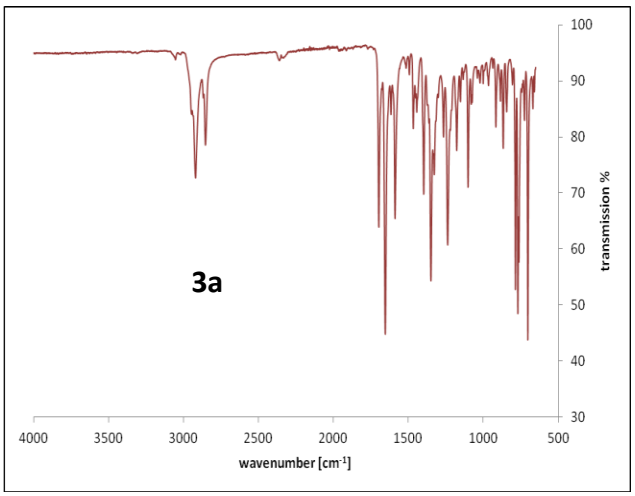
3a
transmission %
wavenumber [cm-1]

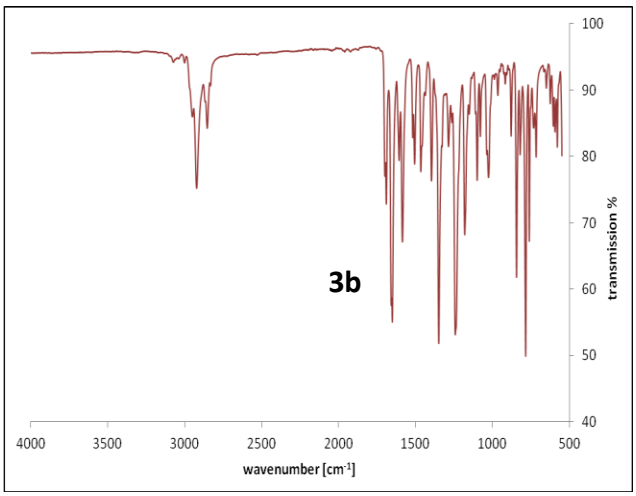
3b
transmission %
wavenumber [cm-1]

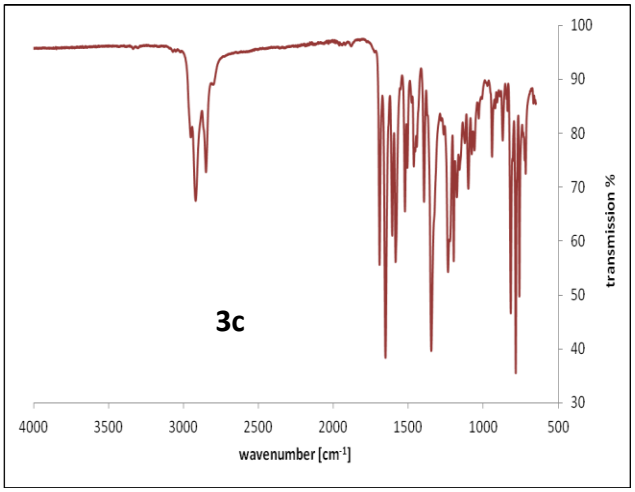
3c
transmission %
wavenumber [cm-1]

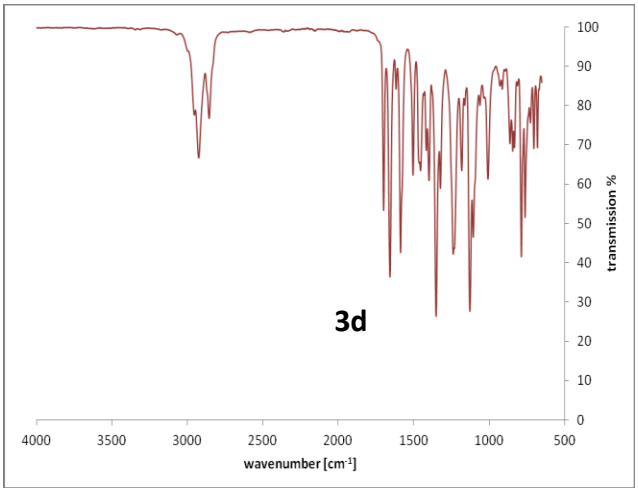
3d
transmission %
wavenumber [cm-1]

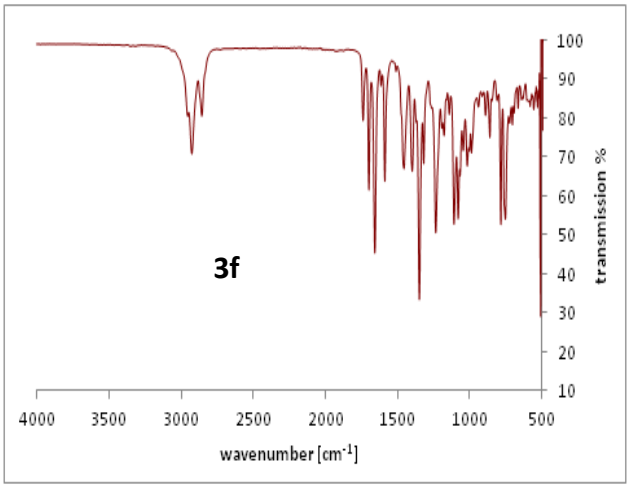
3f
transmission %
wavenumber [cm-1]

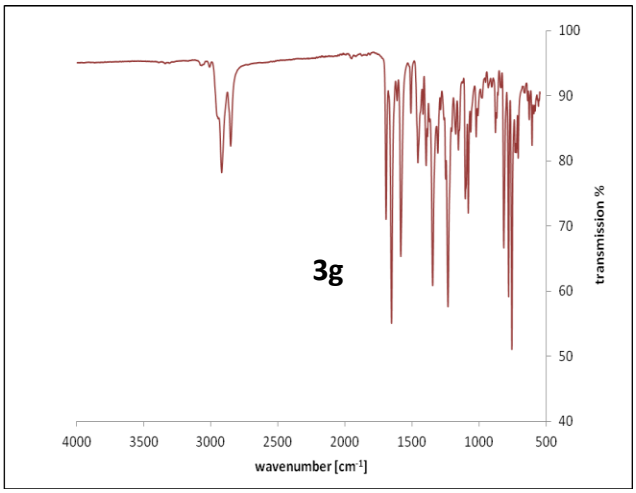
3g
transmission %
wavenumber [cm-1]

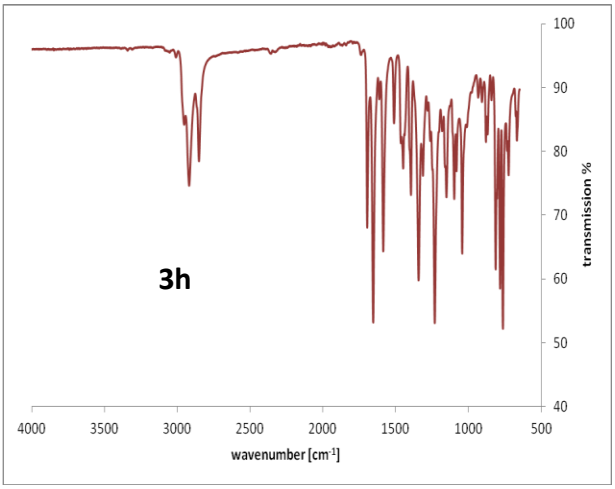
3h
transmission %
wavenumber [cm-1]

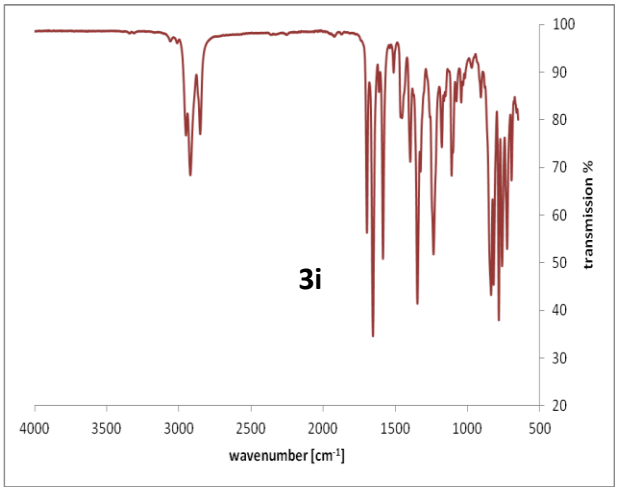
3i
transmission %
wavenumber [cm-1]

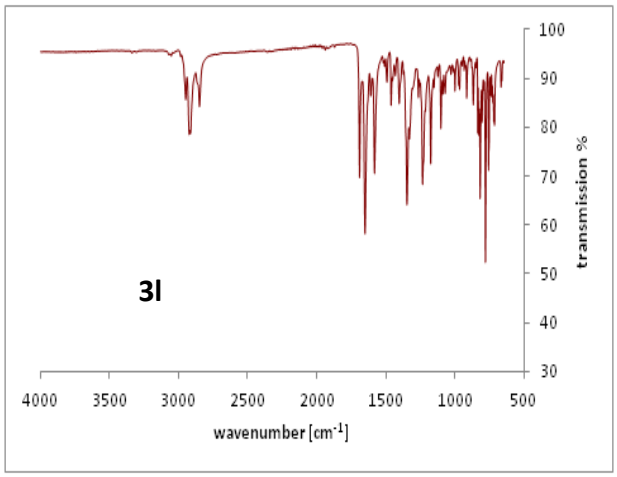
3l
transmission %
wavenumber [cm-1]

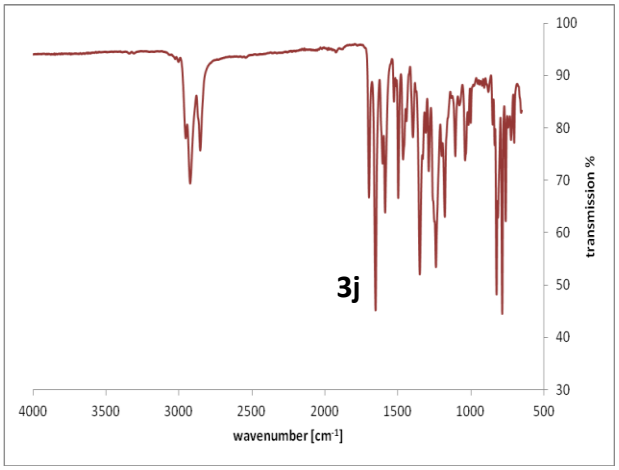
3j
transmission %
wavenumber [cm-1]

7.1. Additional optical spectroscopy data

Table SI-4. Overview of the spectroscopic data.

3a	**CHCl3**	**Tetradecane**	***n*-Hexane**	**1-Butanol**	**1-Undecanol**	**DMF**	**Toluene**
λ_{Abs}[a]	355.4	343.4	342.2	355.2	353.4	355.2	346.8
λ_{Fluo}[b]	420.0	402.3	402.7	429.1	420.6	427.2	410.6
e [c]	17100	17600	16800	19000	18500	17700	16900
Φ [d]	0.78	0.094	0.076	0.95	0.76	0.74	0.50
τ[e]	3.21			3.85		3.62	
3b							
λ_{Abs}[a]	364.8	356.4	354.2	366.2	365.6	368.0	364.2
λ_{Fluo}[b]	459.6	427.8	424.0	498.1	476.4	497.2	443.2
e [c]	16900	15800	15700	17100	16700	16400	16400
Φ [d]	0.83	0.79	0.65	0.83	0.83	0.82	0.75
τ[e]	4.11	3.12	2.65	5.18	4.78	5.24	3.50
3c							
λ_{Abs}[a]	426.2	403.8	401.2	430.2	428.6	433.8	418.2
λ_{Fluo}[b]	578.4	469.8	462.7	638.4	610.0		532.4
e [c]	11200	16500	12300	10300	11800	10700	10800
Φ [d]	0.64	0.73	0.70	0.013	0.14	0.0037	0.65
τ[e]	6.99	3.61	3.47	3.50	5.51		5.12
3d							
λ_{Abs}[a]	362.2	357.0	354.8	361.4	362.6	365.6	360.8
λ_{Fluo}[b]	525.1	442.3	440.2	572.1	526.4	618.8	492.4
e [c]	15900	17100	16500	16600	16900	16500	17000
Φ [d]	0.65	0.51	0.41	0.022	0.26	0.0065	0.71
τ[e]	6.62	2.78	2.03	0.208	1.75	0.119	5.40
3g							
λ_{Abs}[a]	325.0	322.6	322.6	323.6	323.8	323.8	324.0
λ_{Fluo}[b]	509.7	431.7	427.1	576.8	532.4	581.8	478.0
e [c]	15300	16200	14900	16200	18800	15200	16000
Φ [d]	0.39	0.34	0.33	0.088	0.23	0.13	0.18
τ[e]	4.07	1.83	1.70	1.80	4.85	3.85	1.53
3h							
λ_{Abs}[a]	329.0	327.2	326.6	327.8	329.0	328.8	328.8
λ_{Fluo}[b]	522.7	440.2	434.8	570.1	537.0	597.8	487.0
e [c]	17100	16000	16800	18100	15900	17000	16900
Φ [d]	0.40	0.34	0.34	0.047	0.28	0.055	0.19
τ[e]	4.14	1.89	1.88	1.05	3.10	3.01	1.59
3i							
λ_{Abs}[a]	356.0	344.4	343.4	357.6	355.0	356.0	353.4
λ_{Fluo}[b]	425.4	407.0	406.7	434.2	430.6	432.7	416.7
e [c]	18600	18800	17400	18600	19100	17900	18200
Φ [d]	0.79	0.18	0.14	0.89	0.85	0.64	0.51
τ[e]	3.08	5.08		3.63	3.81	3.38	2.03
3j							
λ_{Abs}[a]	366.4	356.2	355.6	367.8	365.8	367.8	364.6
λ_{Fluo}[b]	447.4	410.8	407.4	480.0	457.5	478.3	427.5
e [c]	23700	26400	22600	24100	24600	22800	22400
Φ [d]	0.54	0.54	0.53	0.70	0.71	0.55	0.51
τ[e]	1.34	0.994	1.02	2.21	2.12	2.15	1.16
3l							
λ_{Abs}[a]	364.4	357.6	354.0	366.0	369.4	369.0	364.8
λ_{Fluo}[b]	492.2	436.7	426.8	556.6	518.2	583.4	454.6
e [c]	27500	29300	28300	27500	26800	28300	27500
Φ [d]	0.67	0.50	0.50	0.16	0.56	0.15	0.40
τ[e]	2.93	1.43	1.35	1.05	3.21	1.91	1.40

[a]Absorption maxima in nm; [b]fluorescence maxima in nm; [c] molar extinction coefficients in L mol^{-1} cm^{-1}; [d]fluorescence quantum yields, exc = λ_{max}, reference: *N*,*N*'-Bis(tridecan-7-yl)perylene-3,4:9,10-tetracarboxylic diimide with Φ = 1.00; [e]fluorescence lifetimes in ns.

Table SI-5. FWHM*-values of experimental absorption and fluorescence spectra of **3** in nm.

	n-Hexane		Tetradecane		Toluene		Chloroform		1-Undecanol		1-Butanol		DMF	
	Abs.[a]	**Fluo.[b]**	**Abs.[a]**	**Fluo.[b]**	**Abs.[a]**	**Fluo.[b]**	**Abs.[a]**	**Fluo.[b]**	**Abs.[a]**	**Fluo.[b]**	**Abs.[a]**	**Fluo.[b]**	**Abs.[a]**	**Fluo.[b]**
3a	48.4	58.5	51.6	59.6	52.0	60.2	52.2	63.2	51.8	67.4	48.8	67.7	52.2	66.4
3b	54.4	64.5	53.6	64.4	60.2	70.8	60.4	74.0	58.2	88.0	64.8	90.9	62.8	93.1
3c	76.4	66.2	79.0	70.8	88.4	83.8	85.0	101.0	92.4	164.1	109.4	205.0	93.2	
3d	54.0	70.4	59.6	71.2	62.8	86.6	64.0	104.1	61.8	134.9	66.8	160.1	68.0	
3g	83.8	66.4	76.2	67.1		77.8	81.2	91.6		122.3	83.4	141.5		135.5
3h	79.2	68.2	81.8	67.3		83.5	82.4	95.6	50.6	123.5	82.0	150.0		143.0
3i	50.2	59.2	52.2	60.2	53.0	62.4	53.2	65.9	53.8	70.9	52.2	69.4	53.8	68.2
3j	56.4	57.1	53.2	57.9	52.8	60.7	54.6	71.9	57.9	87.0	58.8	89.0	60.2	90.7
3l	56.4	65.9	57.6	66.6	60.2	74.7	60.4	90.9	63.8	127.1	63.6	154.6	64.2	152.7

*Full width at half maximum, experimental determination. a) FWHM of absorption in eV; b) FWHM of fluorescence in nm.

Table SI-6. FWHM*-values of experimental absorption and fluorescence spectra of **3** in eV.

	n-Hexane		Tetradecane		Toluene		Chloroform		1-Undecanol		1-Butanol		DMF	
	Abs.[a]	**Fluo.[b]**	**Abs.[a]**	**Fluo.[b]**	**Abs.[a]**	**Fluo.[b]**	**Abs.[a]**	**Fluo.[b]**	**Abs.[a]**	**Fluo.[b]**	**Abs.[a]**	**Fluo.[b]**	**Abs.[a]**	**Fluo.[b]**
3a	0.518	0.452	0.552	0.456	0.537	0.434	0.530	0.436	0.531	0.460	0.496	0.444	0.530	0.442
3b	0.546	0.443	0.529	0.435	0.580	0.433	0.571	0.419	0.544	0.466	0.612	0.446	0.590	0.454
3c	0.617	0.360	0.629	0.374	0.657	0.354	0.589	0.359	0.649	0.558	0.781	0.642	0.627	
3d	0.540	0.426	0.594	0.423	0.614	0.429	0.626	0.450	0.593	0.580	0.653	0.606	0.656	
3g	1.011	0.420	0.926	0.419		0.411	0.974	0.423		0.520	1.014	0.518		0.482
3h	0.972	0.415	1.018	0.404		0.426	0.983	0.420	0.547	0.533	0.982	0.553		0.494
3i	0.531	0.445	0.547	0.448	0.542	0.440	0.534	0.441	0.546	0.472	0.526	0.443	0.541	0.444
3j	0.576	0.403	0.531	0.403	0.512	0.395	0.514	0.434	0.547	0.511	0.559	0.471	0.566	0.479
3l	0.567	0.436	0.569	0.433	0.576	0.435	0.568	0.451	0.600	0.584	0.598	0.603	0.601	0.548

*Full width at half maximum, experimental determination. a) FWHM of absorption in eV; b) FWHM of fluorescence in eV.

7.2. Gaussian analysis of the fluorescence spectra of 3g in various solvents

A Gaussian analysis on the basis of equation (SI-8)[SI-7] was applied to the fluorescence spectra of **3g** in the solvents chloroform, *n*-tetradecane, *n*-hexane, 1-butanol, *N*,*N*-dimethylformamide, 1-undecanol and toluene where $I_{(\lambda)}$ means the intensity of fluorescence depending on the wavelengths λ.

$$I_{(\lambda)} = \sum_{i=0}^{n} I_{\max(i)} e^{-100\frac{\left(\frac{1}{\lambda}-\frac{1}{\lambda_{\max(i)}}\right)^2}{2\sigma_{(i)}^2}} \qquad \text{(SI-8)}$$

$$E_{(\lambda)} = \sum_{i=0}^{n} E_{\max(i)} e^{-100\frac{\left(\frac{1}{\lambda}-\frac{1}{\lambda_{\max(i)}}\right)^2}{2\sigma_{(i)}^2}} \qquad \text{(SI-9)}$$

$I_{\max(i)}$ means the intensity maxima of the individual Gaussian bands *i* with the position $\lambda_{\max(i)}$ and the sigma width $\sigma_{(i)}$. The similar equation (SI-9) can be used for the light absorption with the absorptivity *E*. A number of *n* = 8 Gaussian band is sufficient for the description of the fluorescence spectra of the series of **3** reported in Table SI-7. Further Gaussian bands do not improve the results.

Table SI-7. Gaussian analysis of fluorescence spectra of **3g** (300-750 nm).

Solvent	$CHCl_3$	Tetradecane	*n*-Hexane	1-Butanol	DMF	1-Undecanol	Toluene
$\lambda_{max}(1)^{a)}$	365.1	338.2	338.2	357.3	372.4	354.3	373.1
$2\ \sigma^2(1)^{b)}$	4.373	4.477	4.539	0.156	6.189	2.177	2.816
$I_{max}(1)^{c)}$	0.001	0.032	0.004	0.032	0.033	0.067	0.033
$\lambda_{max}(2)^{a)}$	385.0	366.2	361.4	378.6	422.4	394.0	399.3
$2\ \sigma^2(2)^{b)}$	1.803	1.710	1.381	3.445	1.468	4.860	1.639
$I_{max}(2)^{c)}$	0	0.027	0.017	0.137	0.021	0.172	0.013
$\lambda_{max}(3)^{a)}$	405.5	385.4	392.1	409.1	392.4	660.7	410.7
$2\ \sigma^2(3)^{b)}$	4.160	0.696	2.233	6.261	3.521	26.413	12.789
$I_{max}(3)^{c)}$	0.003	0.02	0.027	0.087	0.082	0.035	0.016
$\lambda_{max}(4)^{a)}$	488.0	412.9	410.9	509.7	547.3	457.2	465.2
$2\ \sigma^2(4)^{b)}$	1.695	0.731	0.556	3.446	2.307	4.390	1.455
$I_{max}(4)^{c)}$	0.294	0.183	0.215	0.173	0.585	0.109	0.799
$\lambda_{max}(5)^{a)}$	505.3	423.3	420.0	542.8	594.6	502.7	493.2
$2\ \sigma^2(5)^{b)}$	1.798	0.463	0.362	1.841	1.766	2.805	0.971
$I_{max}(5)^{c)}$	0.637	0.518	0.223	0.54	0.632	0.432	0.431
$\lambda_{max}(6)^{a)}$	535.4	433	428.6	571.7	641.5	538.3	520.5
$2\ \sigma^2(6)^{b)}$	1.094	0.321	0.762	0.956	0.88	2.179	1.364
$I_{max}(6)^{c)}$	0.377	0.153	0.685	0.224	0.164	0.591	0.38
$\lambda_{max}(7)^{a)}$	565.5	449.6	448.6	606.6	678.9	579.2	556.1
$2\ \sigma^2(7)^{b)}$	0.959	1.303	0.662	1.809	0.119	1.379	0.97
$I_{max}(7)^{c)}$	0.219	0.879	0.546	0.608	0.021	0.178	0.069
$\lambda_{max}(8)^{a)}$	596.9	483.1	469.5	648.0	648.3	648.0	585.6
$2\ \sigma^2(8)^{b)}$	1.436	0.762	1.263	0.02	0.019	0.02	1.25
$I_{max}(8)^{c)}$	0.123	0.179	0.323	0.35	0.192	0.05	0.045
$R^{d)}$	0.007	0.010	0.008	0.027	0.015	0.014	0.011

a) Calculated wavelength in nm. b) Line-width in 10^6 cm^{-2} (kK^2). c) Calculated intensity for the global I_{max} = 1.00. d)Residual according to equation (SI-10).

$$\boldsymbol{R} = \sqrt{\int \frac{\left[\boldsymbol{I}(\boldsymbol{\lambda})_{calcd.} - \boldsymbol{I}\ (\boldsymbol{\lambda})_{exp.}\right]^2 \boldsymbol{d\lambda}}{\int \left[\boldsymbol{I}(\boldsymbol{\lambda})_{exp.}\right]^2 \boldsymbol{d\lambda}}} \qquad \text{(SI-10)}$$

Table SI-8. Gaussian analysis of the absorption spectra of **3g** (250-650 nm).

Sovent	$CHCl_3$	Tetradecane	*n*-Hexane	1-Butanol	DMF	1-Undecanol	toluene
$\lambda_{max}(1)^{a)}$	405.7	384.4	389.3	401.1	380.6	385.5	393.4
$2\ \sigma^2(1)^{b)}$	1.435	1.832	1.288	9.886	5.998	4.841	2.677
$E_{max}(1)^{c)}$	0.041	0.317	0.087	0.094	0.376	0.43	0.237
$\lambda_{max}(2)^{a)}$	375.7	358.8	367.3	382.9	351.8	349.0	367.3
$2\ \sigma^2(2)^{b)}$	6.800	1.785	3.126	4.792	0.923	1.374	2.552
$E_{max}(2)^{c)}$	0.405	0.386	0.449	0.3	0.455	0.658	0.314
$\lambda_{max}(3)^{a)}$	356.8	352.3	347.8	350.4	340.4	337.9	352.3
$2\ \sigma^2(3)^{b)}$	0.427	0.140	0.751	1.293	0.517	0.521	0.623
$E_{max}(3)^{c)}$	0.272	0.11	0.408	0.584	0.357	0.319	0.369
$\lambda_{max}(4)^{a)}$	344.3	339.2	336.5	339.5	326.4	324.8	340.4
$2\ \sigma^2(4)^{b)}$	0.630	0.941	0.441	0.360	0.984	0.702	0.574
$E_{max}(4)^{c)}$	0.507	0.599	0.404	0.181	0.478	0.468	0.509
$\lambda_{max}(5)^{a)}$	327.2	322.5	323.1	326.7	306.0	308.8	325.7
$2\ \sigma^2(5)^{b)}$	1.374	0.812	1.042	1.578	7.163	5.948	0.844
$E_{max}(5)^{c)}$	0.55	0.475	0.504	0.532	0.799	0.693	0.482
$\lambda_{max}(6)^{a)}$	303.7	307.9	303.1	302.6	265.7	265.7	306.5
$2\ \sigma^2(6)^{b)}$	6.872	4.238	6.968	7.918	6.26	6.26	6.375
$E_{max}(6)^{c)}$	0.776	0.403	0.798	0.786	0.319	0.319	0.799
$\lambda_{max}(7)^{a)}$	269.6	293.6	267.8	265.7	261.0	261.0	267.8
$2\ \sigma^2(7)^{b)}$	4.382	10.649	8.907	6.26	0.716	0.716	8.907
$E_{max}(7)^{c)}$	0	0.484	0.246	0.319	0.057	0.057	0.246
$\lambda_{max}(8)^{a)}$	266.1	260.5	259.6	261.0	243.0	243.0	259.6
$2\ \sigma^2(8)^{b)}$	5.889	1.499	0.317	0.716	4.463	4.463	0.317
$E_{max}(8)^{c)}$	0.342	0.174	0.058	0.057	0.953	0.953	0.058
$R^{d)}$	0.020	0.025	0.017	0.027	0.014	0.029	0.015

a) Calculated wavelength in nm. b) Line-width in 10^6 cm^{-2} (kK^2). c) Calculated absorptivities for the global E_{max} = 1.00. d) Residual according to equation (SI-10).

The individual spectra and their Gaussian analyses are reported in the subsequent Fig. SI-10 to SI-23.

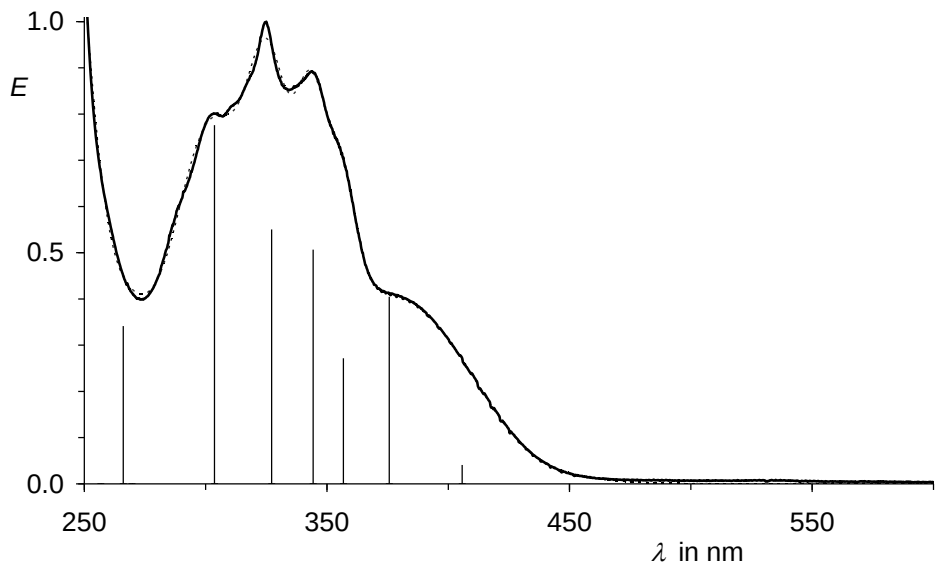

Fig. SI-10. UV/Vis absorption spectrum of **3g** in chloroform normalized to 1 in the UVB (thick, solid curve) and simulated spectrum on the basis of a Gaussian analysis (thin, dashed curve, mainly covered by the experimental spectrum). Bars: Positions and intensities of the individual Gaussian bands.

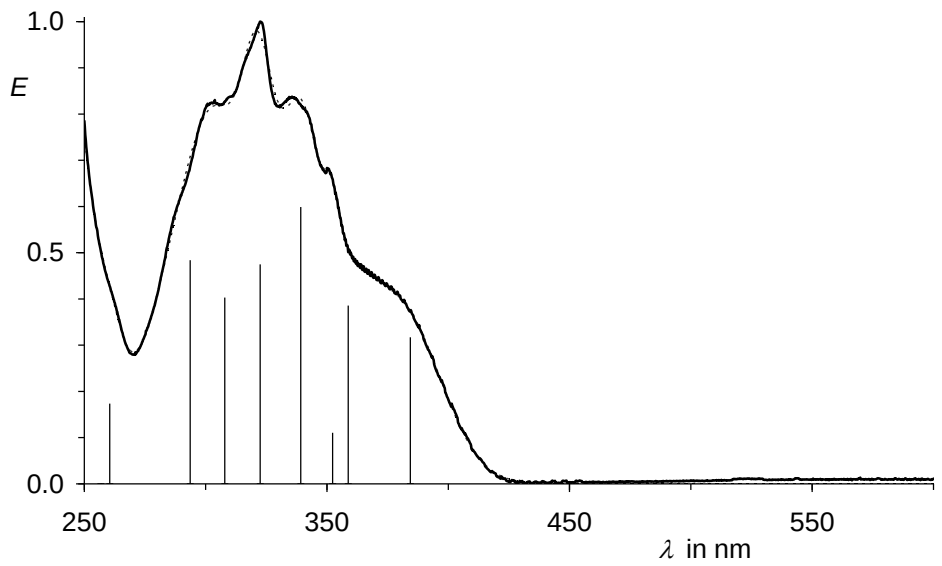

Fig. SI-11. UV/Vis absorption spectrum of **3g** in *n*-tetradecane normalized to 1 in the UVB (thick, solid curve) and simulated spectrum on the basis of a Gaussian analysis (thin, dashed curve, mainly covered by the experimental spectrum). Bars: Positions and intensities of the individual Gaussian bands.

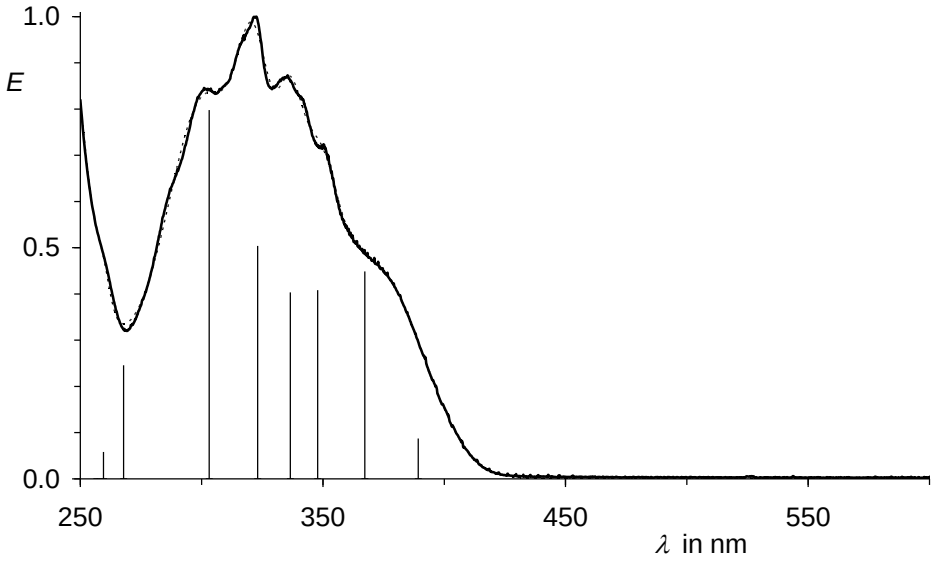

Fig. SI-12. UV/Vis absorption spectrum of **3g** in *n*-hexane normalized to 1 in the UVB (thick, solid curve) and simulated spectrum on the basis of a Gaussian analysis (thin, dashed curve, mainly covered by the experimental spectrum). Bars: Positions and intensities of the individual Gaussian bands.

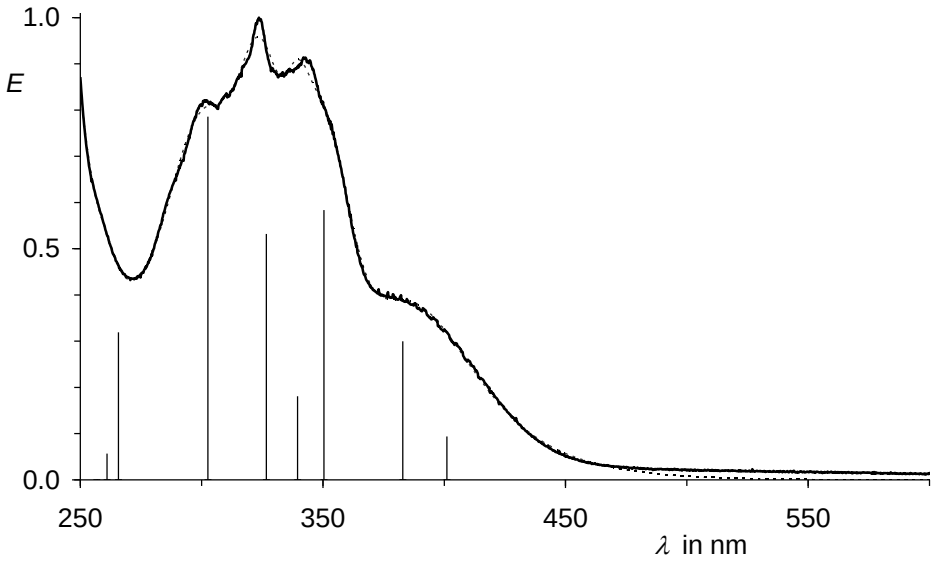

Fig. SI.13. UV/Vis absorption spectrum of **3g** in 1-butanol normalized to 1 in the UVB (thick, solid curve) and simulated spectrum on the basis of a Gaussian analysis (thin, dashed curve, mainly covered by the experimental spectrum). Bars: Positions and intensities of the individual Gaussian bands.

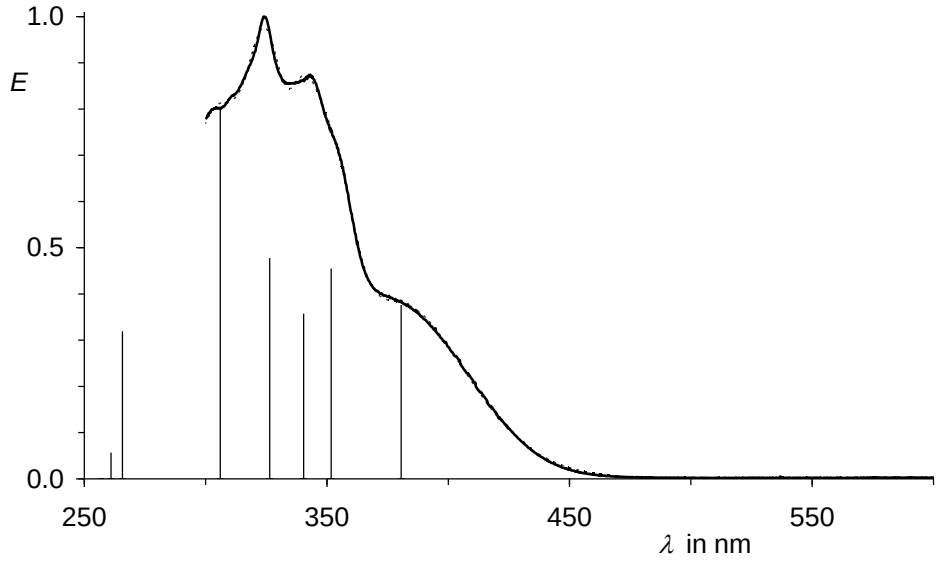

Fig. SI-14. UV/Vis absorption spectrum of **3g** in *N*,*N*-dimethylformamide normalized to 1 in the UVB (thick, solid curve) and simulated spectrum on the basis of a Gaussian analysis (thin, dashed curve, mainly covered by the experimental spectrum). Bars: Positions and intensities of the individual Gaussian bands.

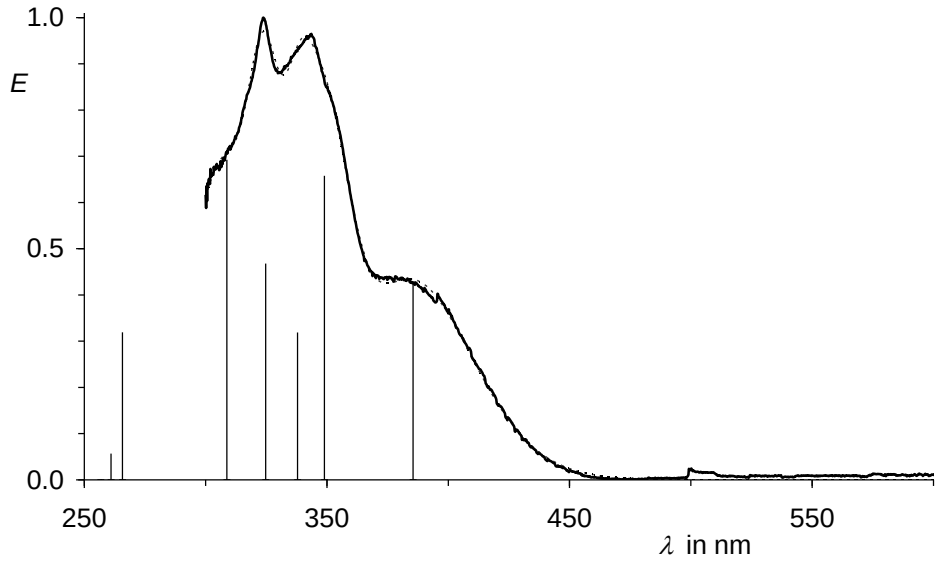

Fig. SI-15. UV/Vis absorption spectrum of **3g** in 1-undecanol normalized to 1 in the UVB (thick, solid curve) and simulated spectrum on the basis of a Gaussian analysis (thin, dashed curve, mainly covered by the experimental spectrum). Bars: Positions and intensities of the individual Gaussian bands.

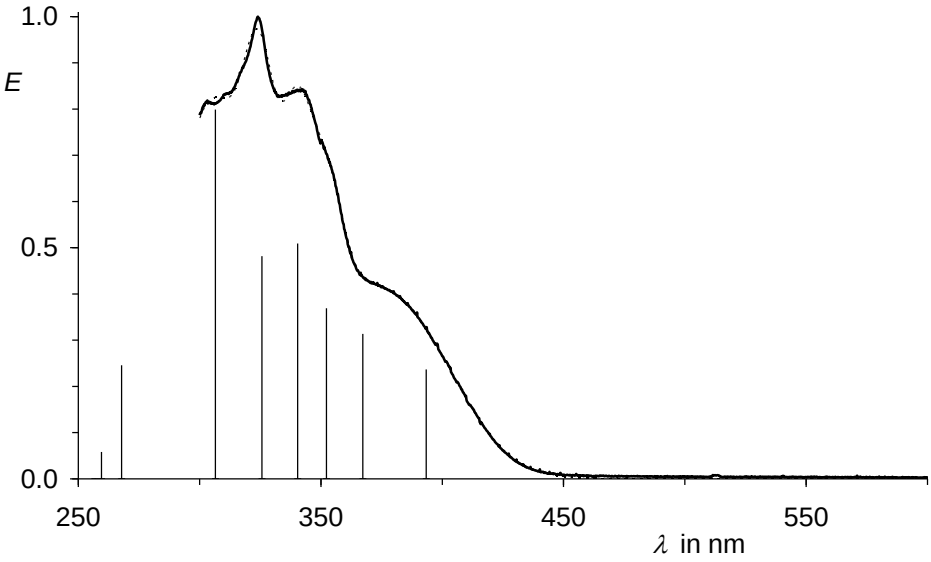

Fig. SI-16. UV/Vis absorption spectrum of **3g** in toluene normalized to 1 in the UVB (thick, solid curve) and simulated spectrum on the basis of a Gaussian analysis (thin, dashed curve, mainly covered by the experimental spectrum). Bars: Positions and intensities of the individual Gaussian bands.

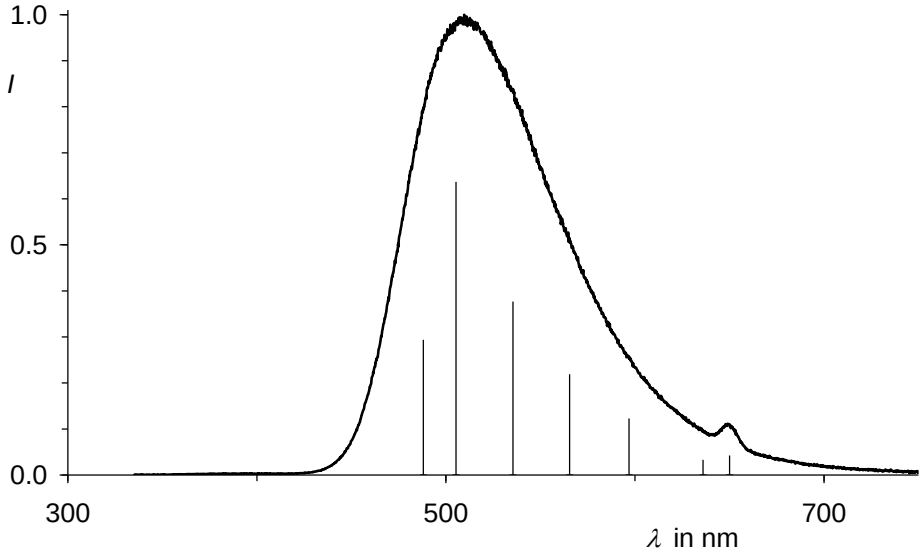

Fig. SI-17. Fluorescence spectrum of **3g** in chloroform normalized to 1 (thick, solid curve) and simulated spectrum on the basis of a Gaussian analysis (thin, dashed curve, mainly covered by the experimental spectrum). Bars: Positions and intensities of the individual Gaussian bands.

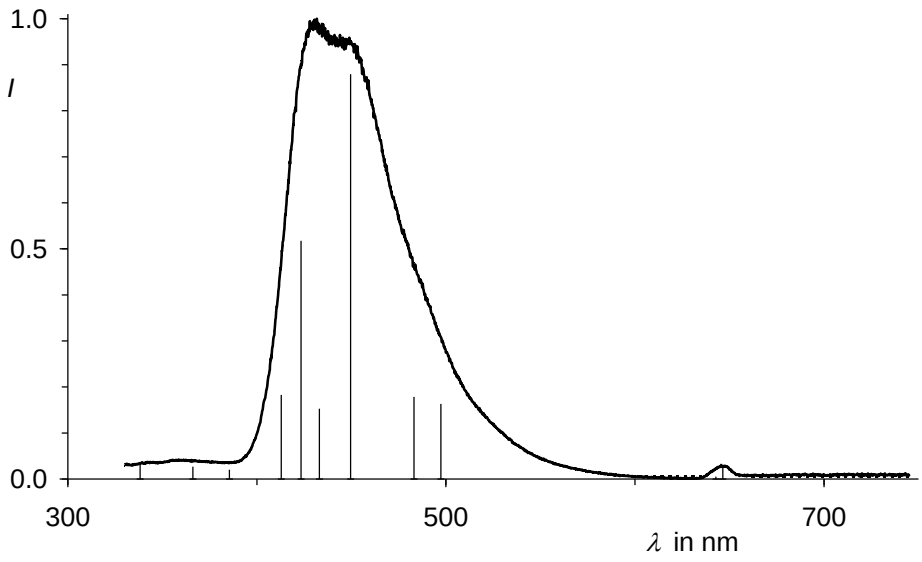

Fig. SI-18. Fluorescence spectrum of **3g** in *n*-tetradecane normalized to 1 (thick, solid curve) and simulated spectrum on the basis of a Gaussian analysis (thin, dashed curve, mainly covered by the experimental spectrum). Bars: Positions and intensities of the individual Gaussian bands.

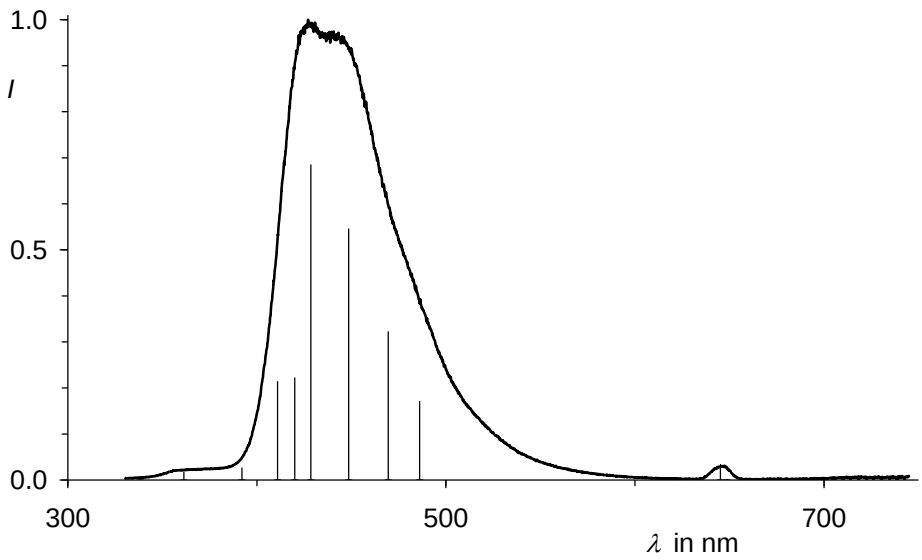

Fig. SI-19. Fluorescence spectrum of **3g** in *n*-hexane normalized to 1 (thick, solid curve) and simulated spectrum on the basis of a Gaussian analysis (thin, dashed curve, mainly covered by the experimental spectrum). Bars: Positions and intensities of the individual Gaussian bands.

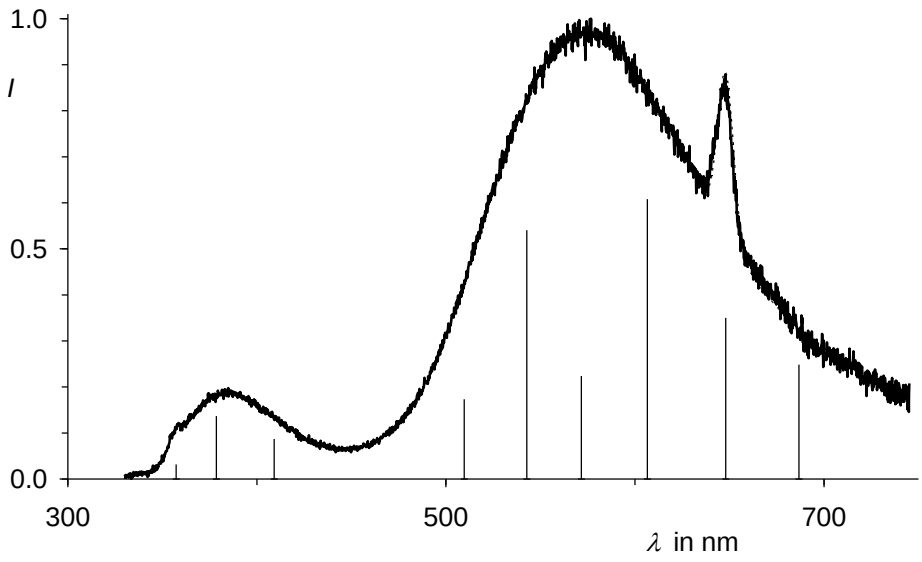

Fig. SI-20. Fluorescence spectrum of **3g** in 1-butanol normalized to 1 (thick, solid curve) and simulated spectrum on the basis of a Gaussian analysis (thin, dashed curve, mainly covered by the experimental spectrum). Bars: Positions and intensities of the individual Gaussian bands. Signal at 648 nm caused by light-scattering of the optical excitation.

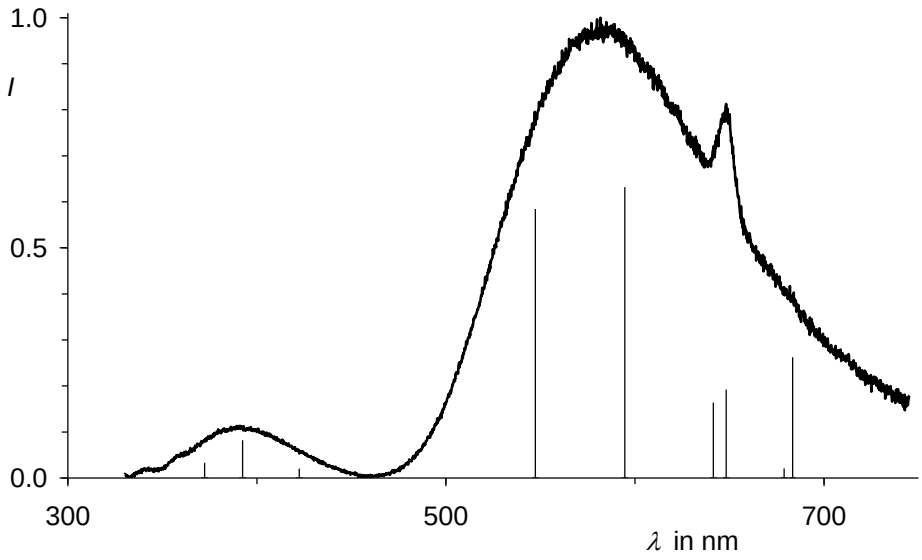

Fig. SI-21. Fluorescence spectrum of **3g** in *N*,*N*-dimethylformamide normalized to 1 (thick, solid curve) and simulated spectrum on the basis of a Gaussian analysis (thin, dashed curve, mainly covered by the experimental spectrum). Bars: Positions and intensities of the individual Gaussian bands. Signal at 648 nm caused by light-scattering of the optical excitation.

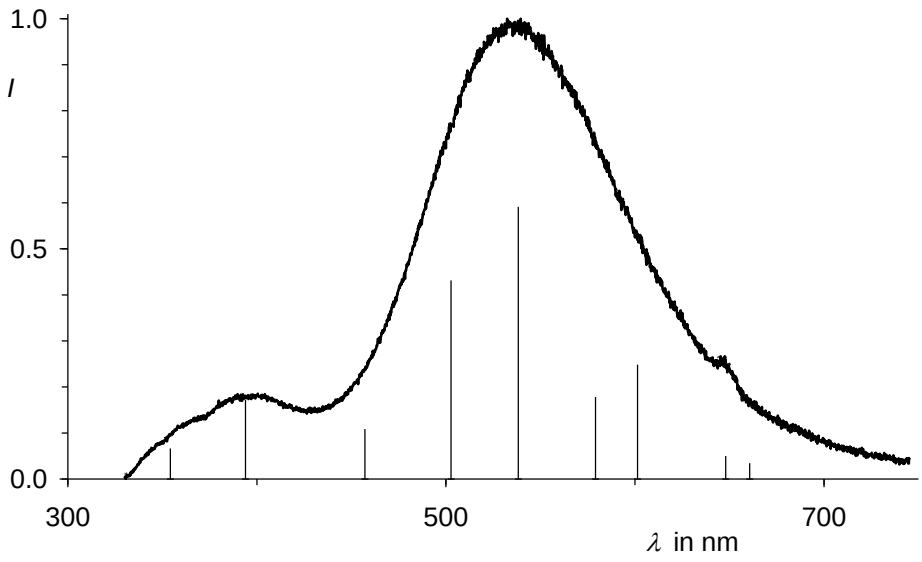

Fig. SI-22. Fluorescence spectrum of **3g** in 1-undecanol normalized to 1 (thick, solid curve) and simulated spectrum on the basis of a Gaussian analysis (thin, dashed curve, mainly covered by the experimental spectrum). Bars: Positions and intensities of the individual Gaussian bands.

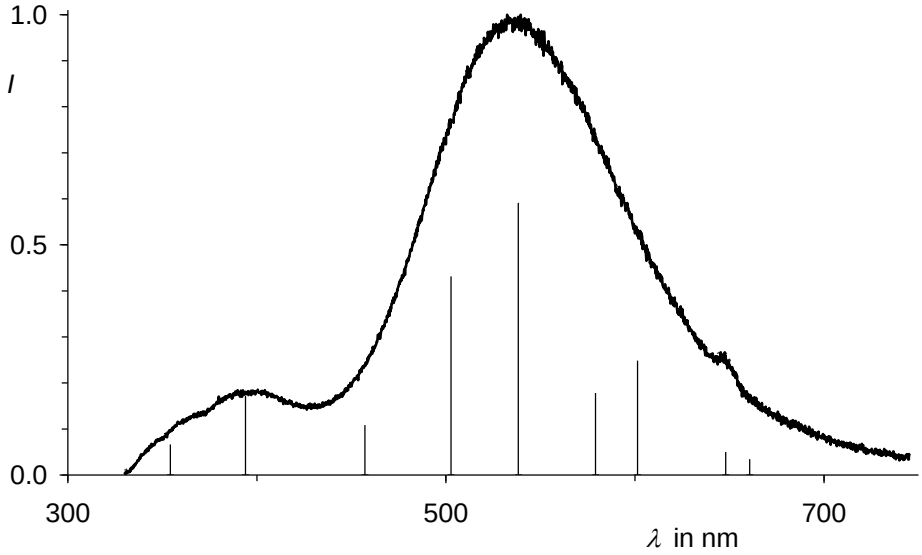

Fig. SI-23. Fluorescence spectrum of **3g** in toluene normalized to 1 (thick, solid curve) and simulated spectrum on the basis of a Gaussian analysis (thin, dashed curve, mainly covered by the experimental spectrum). Bars: Positions and intensities of the individual Gaussian bands.

8. Solvatochromism of 3 according to Dimroth and Reichardt

Table SI-9. Solvatochromism of the fluorescence of **3.**

		1	**2**	**3**	**4**	**5**	**6**	**7**		
Solvent		1-Butanol	$C_{11}H_{22}OH$	DMF	Chloroform	Toluene	*n*-Hexane	Tetradecane	*a*(3-7)[a]	*r*(3-7)[b]
E_T(30)[c]		49.7	47.6	43.2	39.1	33.9	31.0	31.1		
3a	λ_{max}[d]	429.1	420.6	427.2	420.0	410.6	402.7	402.3		
3a	E_T[e]	66.63	67.98	66.93	68.07	69.63	71.00	71.07	-0.34	-0.99
3b	λ_{max}	498.1	476.4	497.2	459.6	443.2	424.0	427.8		
3b	E_T	57.40	60.01	57.50	62.21	64.51	67.43	66.83	-0.74	-0.99
3c	λ_{max}	638.4	610.0		578.4	532.4	462.7	469.8		
3c	E_T	44.79	46.87		49.43	53.70	61.79	60.86	-1.49	-0.96
3d	λ_{max}	572.1	526.4	618.8	525.1	492.4	440.2	442.3		
3d	E_T	49.98	54.31	46.20	54.45	58.06	64.95	64.64	-1.43	-0.98
3g	λ_{max}	576.8	532.4	581.8	509.7	478.0	427.1	431.7		
3g	E_T	49.57	53.70	49.14	56.09	59.81	66.94	66.23	-1.36	-0.98
3h	λ_{max}	570.1	537.0	597.8	522.7	487.0	434.8	440.2		
3h	E_T	50.15	53.24	47.83	54.70	58.71	65.76	64.95	-1.37	-0.99
3i	λ_{max}	434.2	430.6	432.7	425.4	416.7	406.7	407.0		
3i	E_T	65.85	66.40	66.08	67.21	68.61	70.30	70.25	-0.34	-0.99
3j	λ_{max}	480.0	457.5	478.3	447.4	427.5	407.4	410.8		
3j	E_T	59.56	62.49	59.78	63.90	66.88	70.18	69.60	-0.80	-0.99
3l	λ_{max}	556.6	518.2	583.4	492.2	454.6	426.8	436.7		
3l	E_T	51.37	55.17	49.01	58.09	62.89	66.99	65.47	-1.33	-0.98

[a] Slope of the linear correlation between the E_T values and the E_T (30) values for the solvents Nr. 3-7; [b] Correlation number of the linear correlation between the E_T values and the E_T (30) values for the solvents Nr. 3-7; [c] E_T values of the pentaphenylpyridiniumphenolate Nr. 30; [d] fluorescence maxima in nm; [e] molar energy of fluorescence emission in kcal/mol.

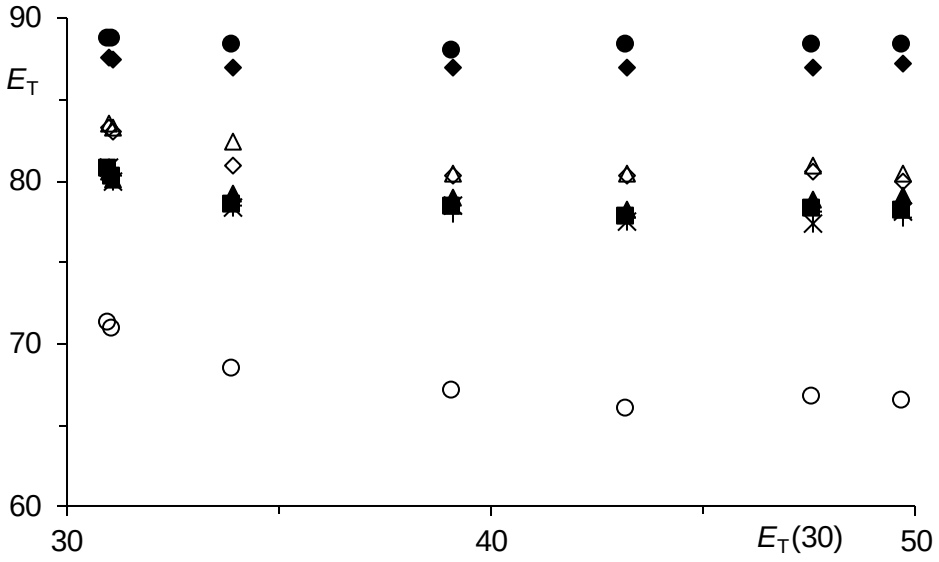

Fig. SI-24. Weak solvatochromism of the absorption of naphthalimides as indicated by plots with the $E_T(30)$ values in kcal/mol. $E_T = 28591/\lambda_{max}$ (absorption in kcal). From left to right: Solvents *n*-hexane, *n*-tetradecane, toluene, chloroform, dimethylformamide, 1-undecanol and 1-butanol. Filled circles **3g**, filled squares **3b**, filled triangles **3d**, filled diamonds **3h**, stars **3l**, open diamonds **3i**, crosses **3j**, open circles **3c**, open triangles **3a**.

9. Additional optical spectra

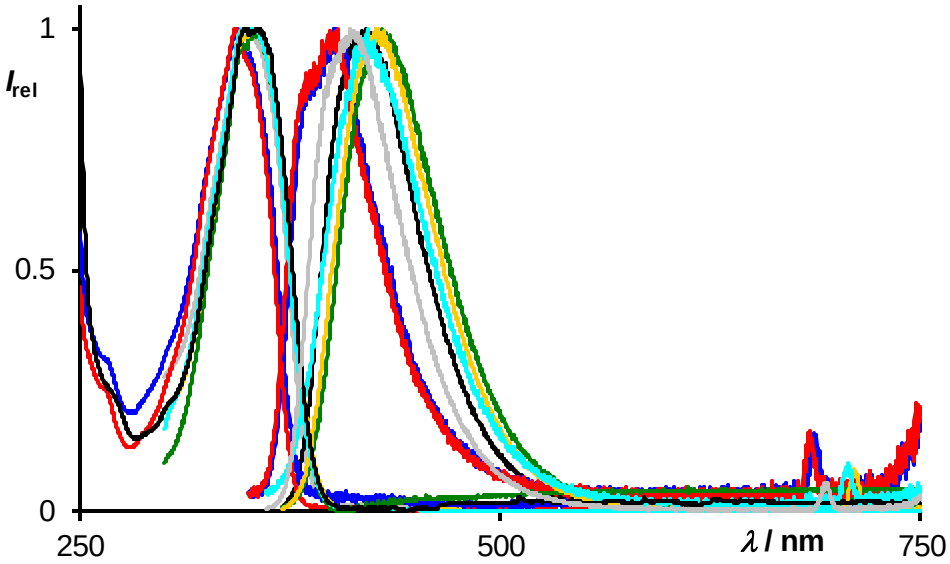

Fig. SI-25. Absorption and fluorescence spectra of **3a**. Applied solvents: *n*-hexane (red), *n*-tetradecane (blue), toluene (grey), chloroform (black), 1-undecanol (turquoise) DMF (yellow), 1-butanol (green).

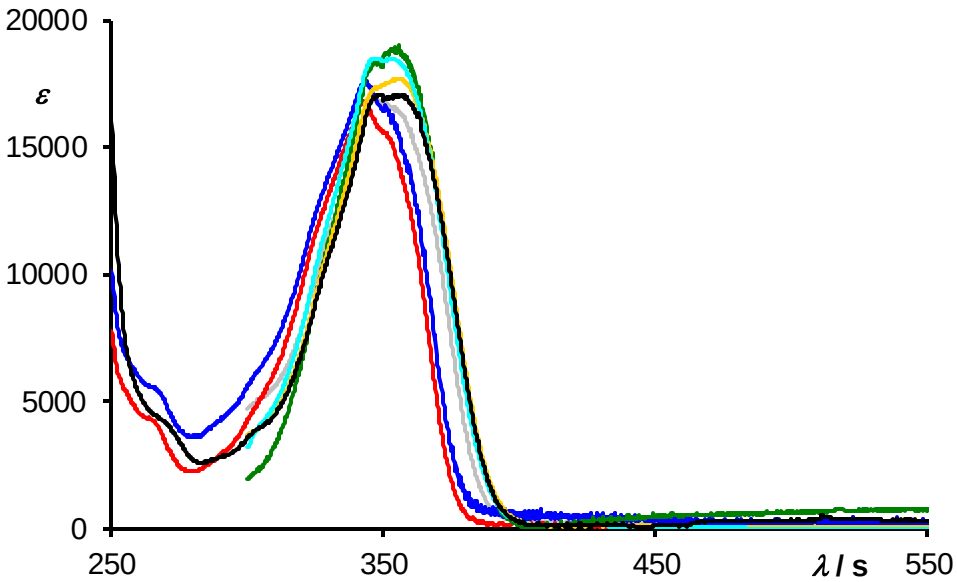

Fig. SI-26. Absolute absorption spectra of **3a**. Molar extinction is given in L mol^{-1} cm^{-1}. Applied solvents: *n*-hexane (red), *n*-tetradecane (blue), toluene (grey), chloroform (black), 1-undecanol (turquoise) DMF (yellow), 1-butanol (green).

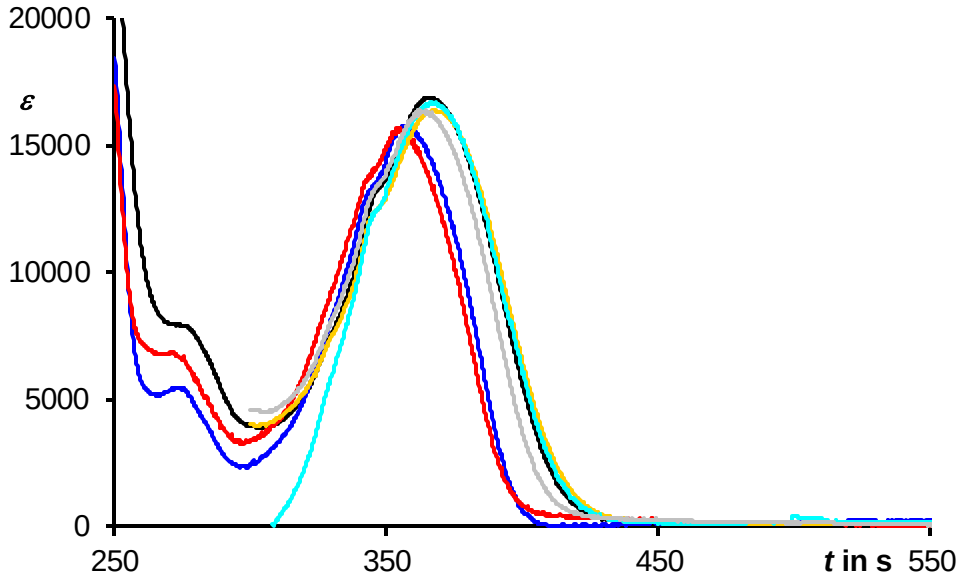

Fig. SI-27. Absolute absorption spectra of **3b**. Molar extinction is given in L mol^{-1} cm^{-1}. Applied solvents: *n*-hexane (red), *n*-tetradecane (blue), toluene (grey), chloroform (black), 1-undecanol (turquoise) DMF (yellow), 1-butanol (green).

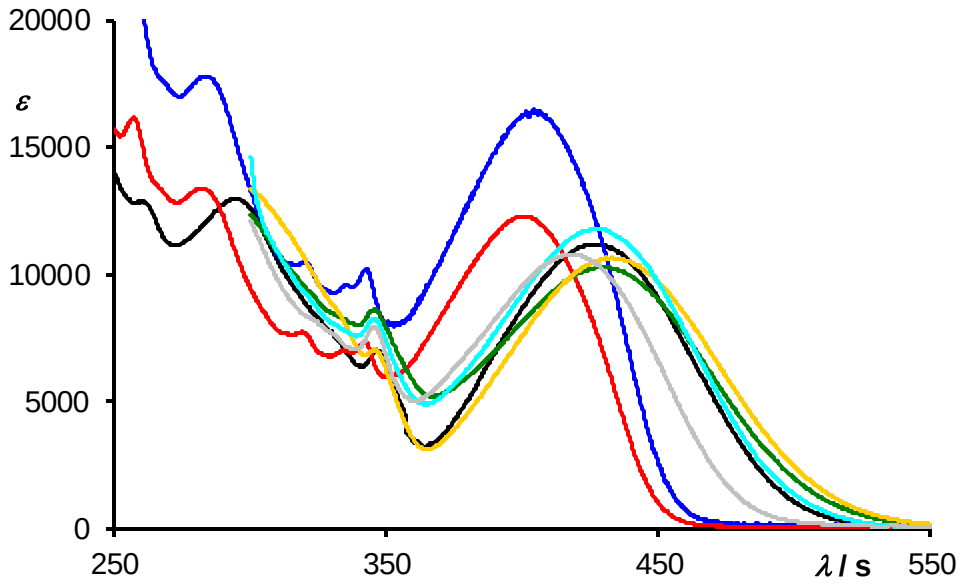

Fig. SI-28. Absolute absorption spectra of **3c**. Molar extinction is given in L mol^{-1} cm^{-1}. Applied solvents: *n*-hexane (red), *n*-tetradecane (blue), toluene (grey), chloroform (black), 1-undecanol (turquoise) DMF (yellow), 1-butanol (green).

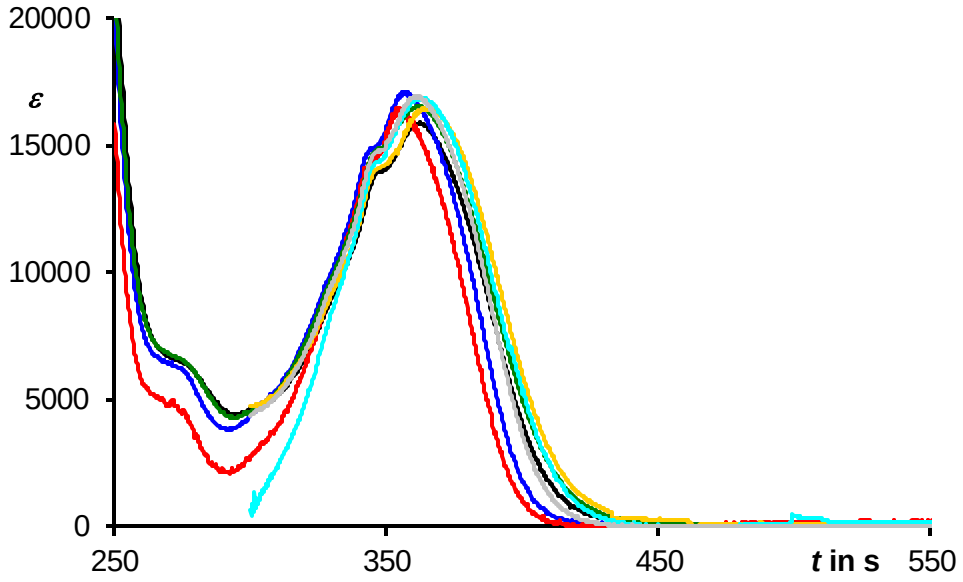

Fig. SI-29. Absolute absorption spectra of **3d**. Molar extinction is given in L mol^{-1} cm^{-1}. Applied solvents: *n*-hexane (red), *n*-tetradecane (blue), toluene (grey), chloroform (black), 1-undecanol (turquoise) DMF (yellow), 1-butanol (green).

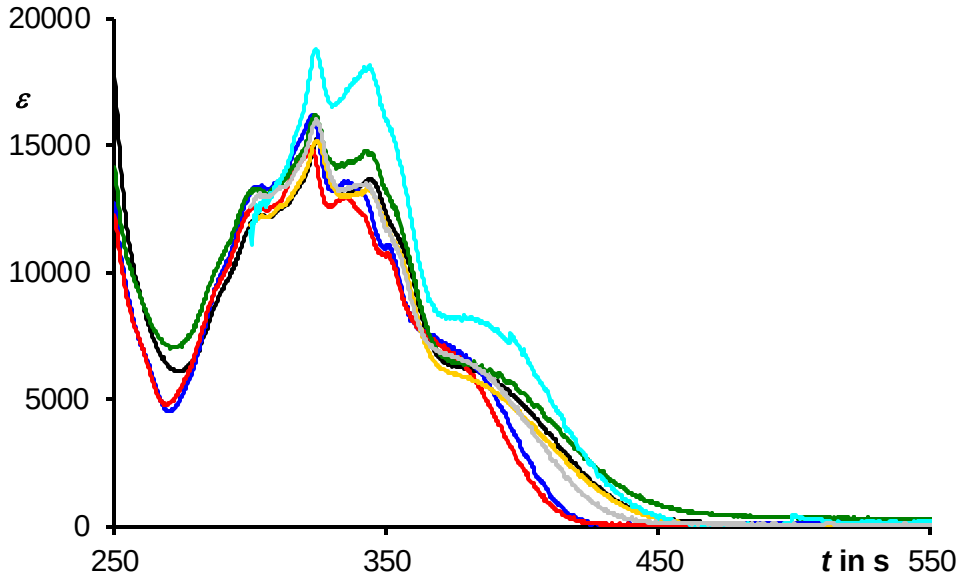

Fig. SI-30. Absolute absorption spectra of **3g**. Molar extinction is given in L mol^{-1} cm^{-1}. Applied solvents: *n*-hexane (red), *n*-tetradecane (blue), toluene (grey), chloroform (black), 1-undecanol (turquoise) DMF (yellow), 1-butanol (green).

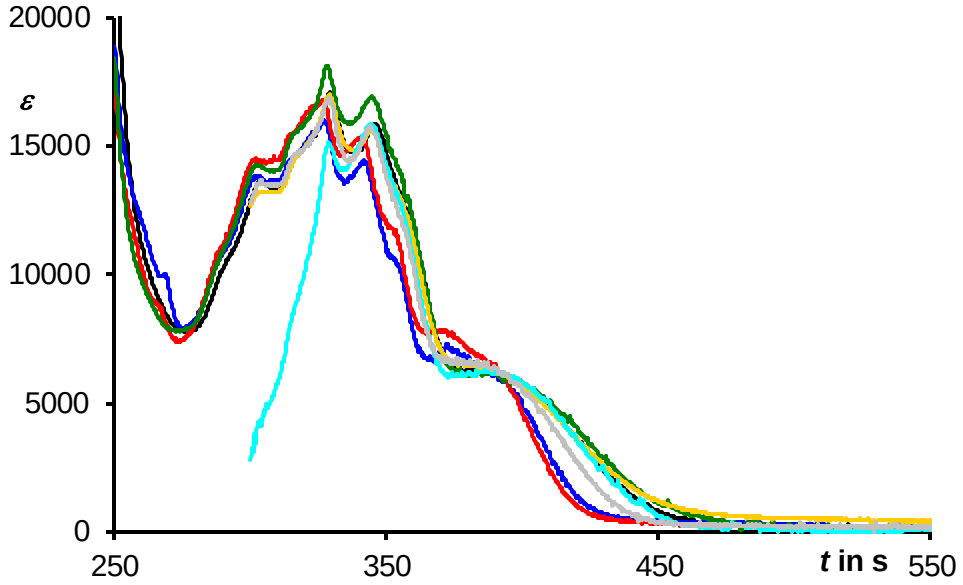

Fig. SI-31. Absolute absorption spectra of **3h**. Molar extinction is given in L mol^{-1} cm^{-1}. Applied solvents: *n*-hexane (red), *n*-tetradecane (blue), toluene (grey), chloroform (black), 1-undecanol (turquoise) DMF (yellow), 1-butanol (green).

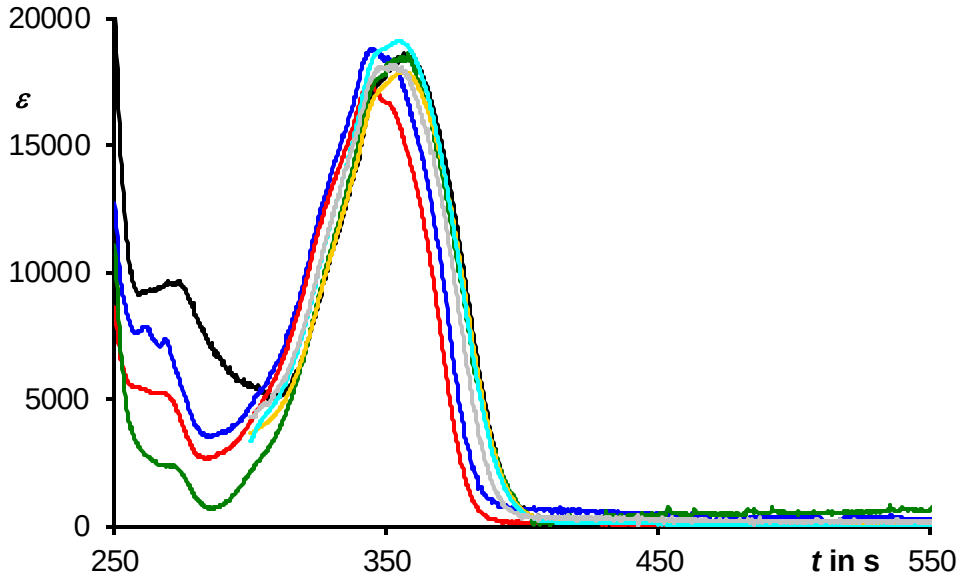

Fig. SI-32. Absolute absorption spectra of **3i**. Molar extinction is given in L mol^{-1} cm^{-1}. Applied solvents: *n*-hexane (red), *n*-tetradecane (blue), toluene (grey), chloroform (black), 1-undecanol (turquoise) DMF (yellow), 1-butanol (green).

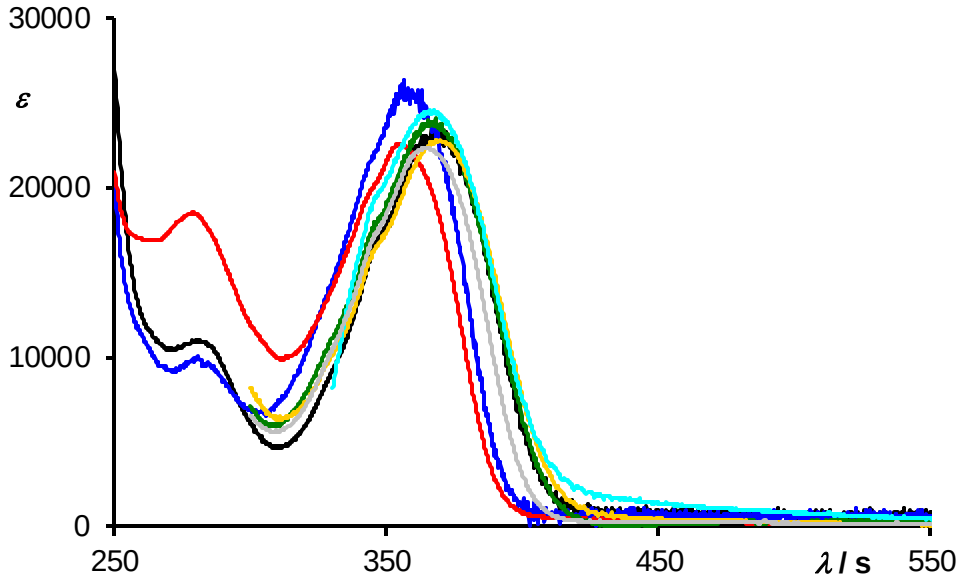

Fig. SI-33. Absolute absorption spectra of **3j**. Molar extinction is given in L mol^{-1} cm^{-1}. Applied solvents: *n*-hexane (red), *n*-tetradecane (blue), toluene (grey), chloroform (black), 1-undecanol (turquoise) DMF (yellow), 1-butanol (green).

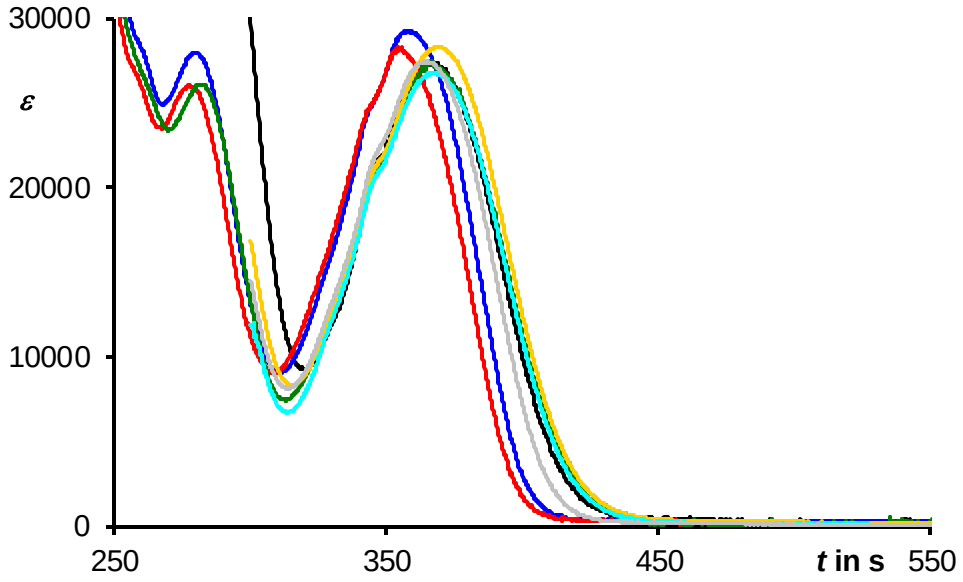

Fig. SI-34. Absolute absorption spectra of **3l**. Molar extinction is given in L mol^{-1} cm^{-1}. Applied solvents: *n*-hexane (red), *n*-tetradecane (blue), toluene (grey), chloroform (black), 1-undecanol (turquoise) DMF (yellow), 1-butanol (green).

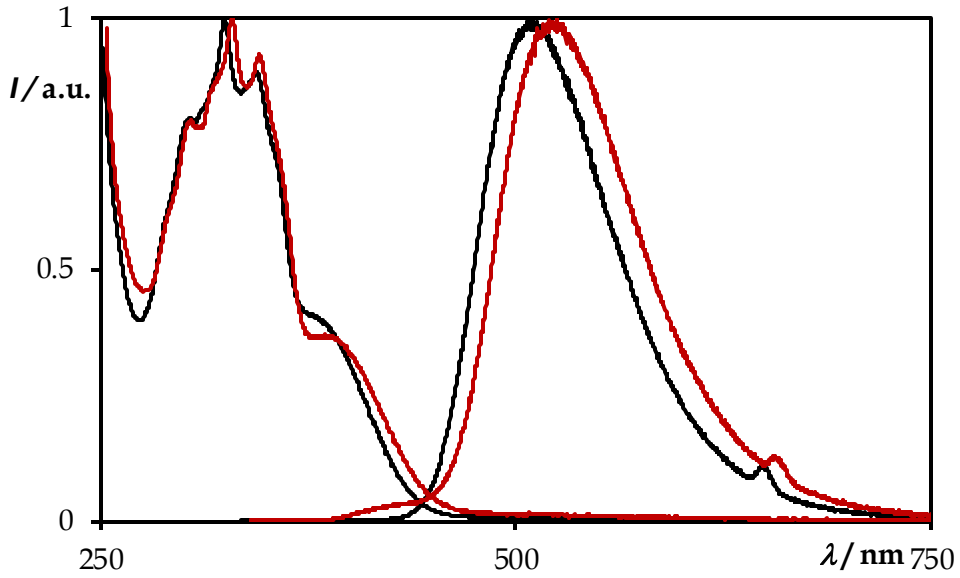

Fig. SI-35. Comparison of absorption (left) and fluorescence (right) spectra of **3g** (black) and **3h** (red) in $CHCl_3$.

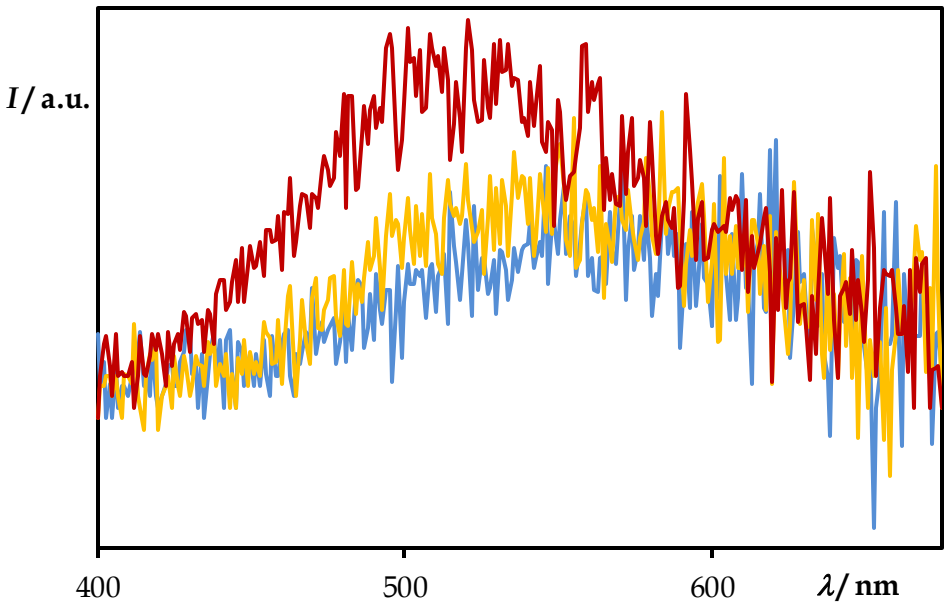

Fig. SI-36. Temperature dependent fluorescence spectra of **3f** in diethylene glycol diethyl ether. Room temperature (blue), approx. 100 °C (yellow), reflux, approx. 200 °C (red).

10. Quantum chemical calculations

Table SI-10. Calculated energies of HOMO and LUMO and comparison to experimental data of **3**.

Dye	E_{HOMO}[a]	E_{LUMO}[a]	$E_{HOMO}(E_1)$[b]	$E_{LUMO}(E_1)$[b]	E_{abs}[c]	λ_{abs} (calc.)[d]	λ_{abs} (meas.)[e]
3a	-6.667	-2.884	-8.027	0.082	3.782383	327.8	355.4
3b	-6.395	-2.803	-7.771	0.166	3.591903	345.2	364.8
3c	-5.606	-2.667	-7.211	0.354	2.93883	421.9	426.2
3d	-6.340	-2.857	-7.837	0.082	3.483057	356.0	362.2
3g	-6.095	-2.830	-7.510	0.245	3.265366	379.7	325.0
3f	-6.177	-2.857	-7.592	0.082	3.319789	373.5	364.4
3h	-5.987	-2.830	-7.347	0.272	3.156521	392.8	329.0
3i	-6.640	-2.857	-7.946	0.082	3.782383	327.8	356.0
3j	-6.993	-3.184	-8.354	-0.327	3.809594	325.5	366.4
3l	-6.531	-2.857	-8.296	0.199	3.673537	337.5	344.8

Applied solvents: *n*-tetradecane, *n*-hexane, toluene, chloroform, dimethylformamide (DMF); a) Calculated energy of HOMO and LUMO in eV in the electronic ground state, respectively (B3LYP 6-331**G); b) Calculated energy of HOMO and LUMO in eV in the electronically excited state, respectively (CIS B3LYP 6-331**G); c) Calculated energetic HOMO-LUMO difference in eV (DFT B3LYP 6-311**G); d) Calculated energetic HOMO-LUMO difference in nm; e) Experimentally determined absorption maxima in chloroform.

Table SI-11 Quantumchemical calculations of **3**.

	Struct. E_0[a]	**Struct. E_1[b]**	**HOMO E_0[c]**	**LUMO E_0[d]**	**HOMO E_1[e]**	**LUMO E_1[f]**
3a	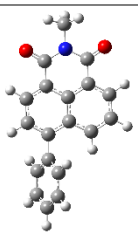	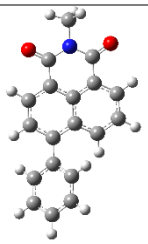	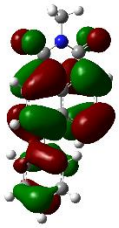	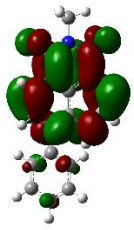	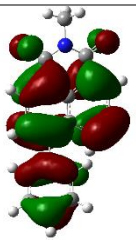	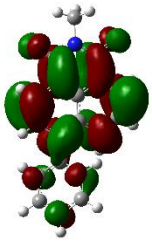
3 b	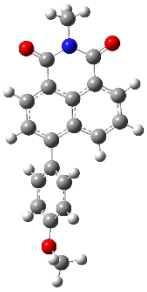	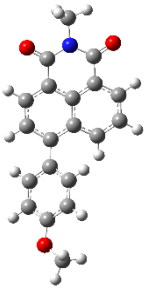	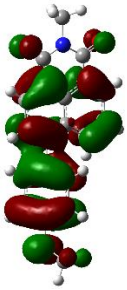	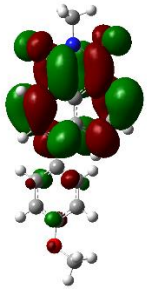	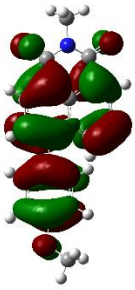	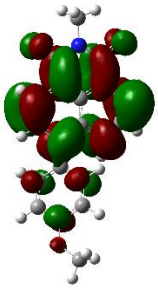
3c	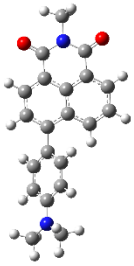	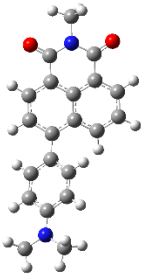	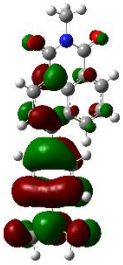	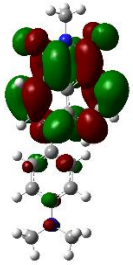	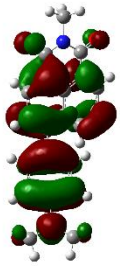	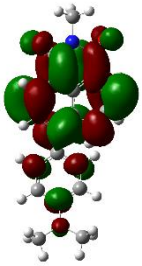
3 d	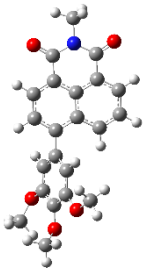	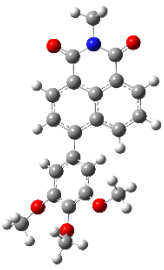	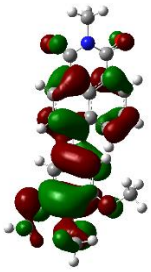	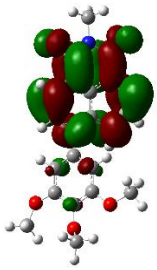	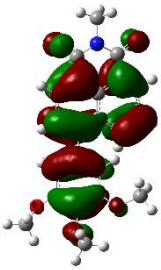	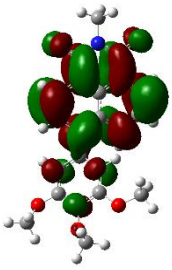
3f	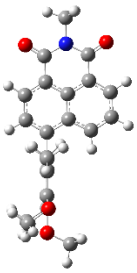	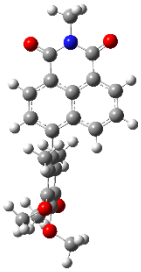	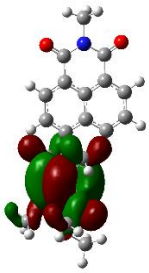	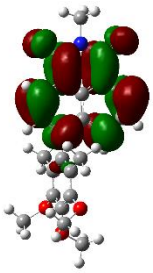	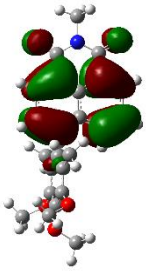	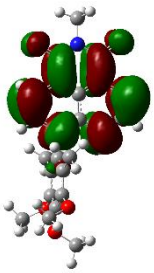

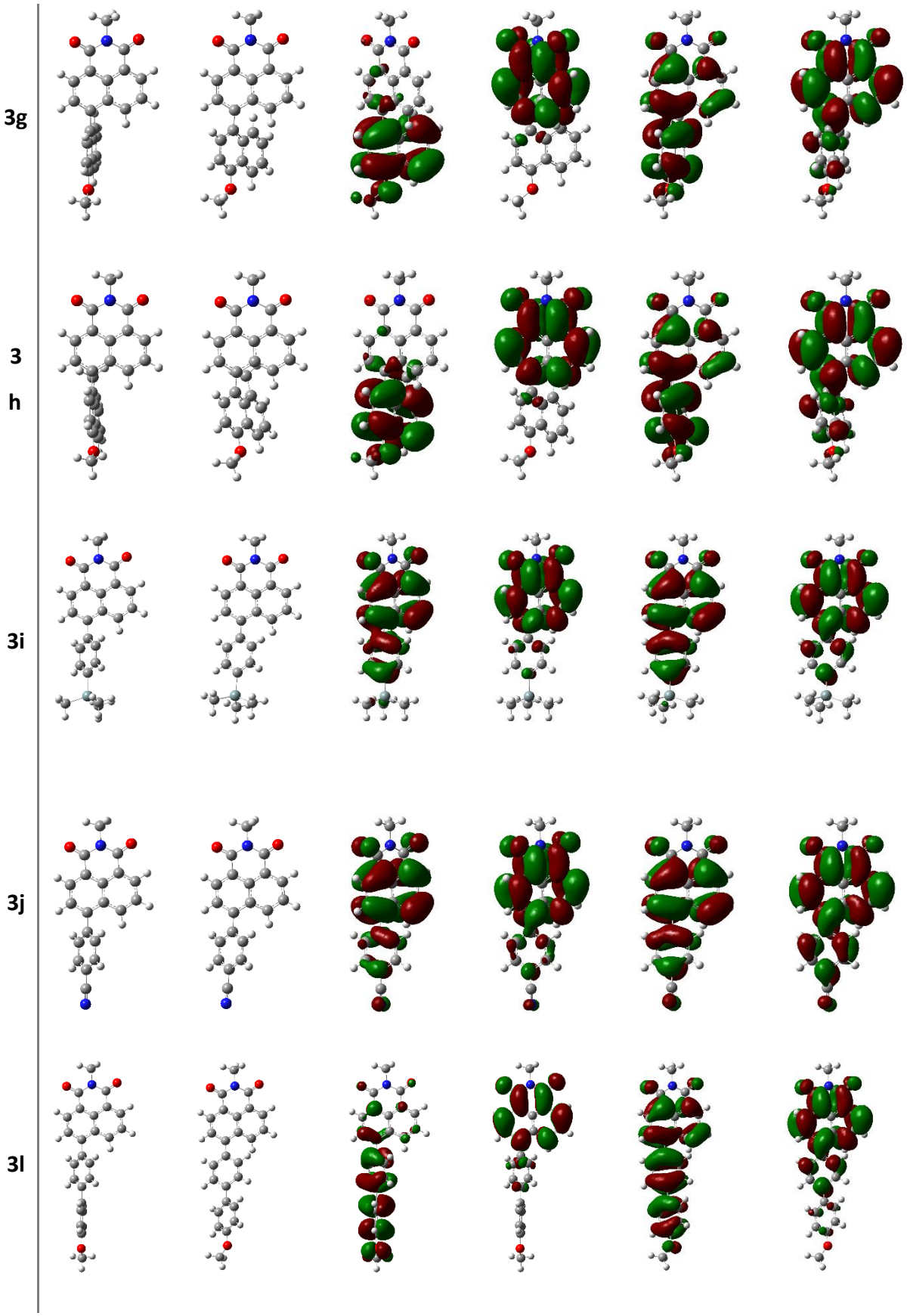

Optimized structures and electron density of HOMO and LUMO (DFT B3LYP 6-311**G and CIS 6-311**G basis set). a) Optimized structure in electronic groundstate; b) Optimized structure in electronically excited state; c) HOMO in groundstate; d) LUMO in ground state; e) HOMO in excited state; f) LUMO in excited state.

11. References

SI-1 A. K. Banerjee, P. S. Poon, M. S. Laya, J. A. Azocar, *Russ. J. Gen. Chem.*, 2003, **73**, 1815.

SI-2 a) Y. Cai, Z. Guo, J. Chen, W. Li, L. Zhong, Y. Gao, L. Jiang, L. Chi, H. Tian, W.-H. Zhu, J. *Am. Chem. Soc.*, 2016, **138**, 2219; b) T. Ishiyama, M. Murata, N. Miyaura, *J. Org. Chem.*, 1995, **60**, 7508.

SI-3 H. Langhals, A. Hofer, *Ger. Offen.* (2014), DE 102012023247 A1 20140626, *Chem. Abstr.*, 2014, **161**, 159273; *PCT Int. Appl.* (2014), WO 2014083011 A2 20140605, *Chem. Abstr.*, 2014, **161**, 43086.

SI-4 A. Kawski, P. Bojarski, B. Kukliński, *Chem. Phys. Lett.*, 2008, **463**, 410.

SI-5 J.-L. M. Abboud, R. W. Taft, M. J. Kamlet, *J. Chem. Soc. Perkin Trans. II*, 1985, 815.

SI-6 J. Catalán, *J. Phys. Chem. B*, 2009, **113**, 5951.

SI-7 H. Langhals, *Anal. Bioanal. Chem.*, 2002, **374**, 573.